The Effects of UV Irradiation on the Biosorption of Titanium Dioxide Nanoparticles to Heterotrophic Biomass

by

William Mark Young Jr

A THESIS

submitted to

Oregon State University

Honors College

in partial fulfillment of
the requirements for the
degree of

Honors Baccalaureate of Science in Environmental Engineering
(Honors Scholar)

Presented June 1, 2017
Commencement June 2017

AN ABSTRACT OF THE THESIS OF

William Mark Young Jr. for the degree of Honors Baccalaureate of Science in Environmental Engineering presented on June 1, 2017.

Title: The Effects of UV Irradiation on the Biosorption of Titanium Dioxide Nanoparticles to Heterotrophic Biomass

Abstract approved: _____

Jeffrey A. Nason

The production of titanium dioxide (TiO_2) nanoparticles has increased significantly in the past decades, which has generated concern due to their known toxicity in the environment. As a result of the production, use and disposal of productions containing TiO_2, TiO_2 nanoparticles are often received by wastewater treatment facilities. The adsorption of TiO_2 nanoparticle to heterotrophic biomass has been previously studied; however, past studies did not address the effects of environmental transformations of the nanoparticles' surface properties. These changes often occur in the environment prior to being received by the wastewater treatment facility. This study uses gold labeled TiO_2 ($Au@TiO_2$) nanoparticles to observe how exposure to ultraviolet (UV) irradiation modifies the surface properties of TiO_2 nanoparticles, and ultimately affects their adsorption to heterotrophic biomass. Using instrumental neutron activation analysis, the limit of detection and the limit of quantification of $Au@TiO_2$ nanoparticles in dried return activated sludge was found to be 5.49 mg/kg 7.02 mg/kg, respectively. These values are high due to the relatively large amount of background Au in the return activated sludge (24.0 µg/L). Exposure to UV irradiation reduced $Au@TiO_2$ nanoparticle hydrophobicity and shifted the electrophoretic mobility versus pH curve to the left. Batch adsorption tests were used to quantify biosorption of $Au@TiO_2$ nanoparticles to heterotrophic biomass. Analysis of Au in the supernatant and the settled solids from the batch adsorption tests yielded an incomplete material balance. The Au concentration of the supernatant suggested that exposure to UV irradiation increased biosorption to heterotrophic biomass. However, using the Au measured in settled solids, no relationship between exposure to UV irradiation and biosorption was observed. Further analysis is necessary to close the material balance and determine the effects of UV irradiation on biosorption.

Key Words: TiO_2, Nanoparticles, Wastewater, Ultraviolet, Biosorption
Corresponding e-mail address: william.young2150@gmail.com

The Effects of UV Irradiation on the Biosorption of Titanium Dioxide Nanoparticles to Heterotrophic Biomass

by

William Mark Young Jr.

A THESIS

submitted to

Oregon State University

University Honors College

in partial fulfillment of
the requirements for the
degree of

Honors Baccalaureate of Science in Environmental Engineering
(Honors Scholar)

Presented June 1, 2017
Commencement June 2017

Honors Bacclaureate of Science in Environmental Engineering project of William Young presented on June 1, 2017

APPROVED:

Jeffrey Nason, Mentor, representing Environmental Engineering

---

Tyler Radniecki, Committee member, representing Environmental Engineering

---

Alyssa Deline, Committee member, representing Environmental Engineering

---

Toni Doolen, Dean, University Honors College

I understand that my thesis will become part of the permanent collection of Oregon State University, University Honors College. My signature below authorizes release of my thesis to any reader upon request.

William Mark Young Jr., Author

Table of Contents

List of Figures

ACKNOWLEDGMENTS

I would like to thank my advisor Dr. Jeff Nason for his guidance and allowing me to be a part of such an interesting project. In addition, I would like to thank my mentor Alyssa Deline for the endless support I received over the past four years and for the enormous amount that she has taught me throughout this project. I would like to thank Dr. Leah Minc for conducting the instrumental neutron activation analysis. Thank you Dr. Tyler Radniecki for being a member of my thesis committee. Additional thanks to fellow lab-mates Dan Pike, Michael Kelly, Jason Silvertooth, Brian Rowbotham Sarah Burch, Mark Surette, Brent Deyo, Joy-Marie Gerould, Jasmin Kennard, Isabella Lewis, Aubrey Dondick, Ariel Mosbrucker, Jessica Steigerwald, Justine Feist, Monce Barajas and Kelly Hollenbeck for support. Thank you Pete and Rosalie Johnson, the DeLoach Work Scholarship and NSF Grant 1255020 for providing funding that made this opportunity possible. Finally, a huge thanks to my friends and family for encouraging and supporting me through the entire process.

1 Introduction

1.1 Motivation

The production and application of engineered nanomaterials, specifically titanium dioxide (TiO_2) nanoparticles, has increased considerably over the past decade and is expected to continue to increase.[1] Engineered TiO_2 nanoparticles are used in a variety of products such as sunscreens, cosmetics, paints and self-cleaning surfaces that utilize the particles' photocatalytic activity, white color, and ultraviolet (UV) absorbing properties.[200] This has caused anthropogenic TiO_2 nanoparticles to be measured in natural waters, runoff and wastewater treatment plants at levels higher than normal background concentrations.[54] This is problematic because the presence and accumulation of TiO_2 nanoparticles has also been associated with negative environmental and human health effects, such as being toxic to various aquatic species, inhibiting nitrifying bacteria in wastewater treatment plants and causing respiratory stress when inhaled.[2, 15,17] These factors demonstrate the importance of understanding the ultimate fate and transport of TiO_2 nanoparticles when released into environmental matrices.

Many applications of TiO_2 nanoparticles either directly or indirectly cause them to be received in a municipal wastewater treatment facility. Westerhoff et al. observed that 96% of influent Ti is removed by wastewater treatment plants. However, analysis of wastewater effluent found that some TiO_2 nanoparticles were able to pass through wastewater treatment plants and enter aquatic systems.[24] The removal of TiO_2 nanoparticles in wastewater treatment has been studied by observing their biosorption to heterotrophic biomass, a major component of activated sludge. Once sorbed by the biomass, TiO_2 nanoparticles are removed by settling in secondary clarification. Kiser et al. performed a batch adsorption isotherm experiment and modeled TiO_2 nanoparticle biosorption with a Freundlich adsorption isotherm.[35] This study provides valuable information concerning the removal of TiO_2 nanoparticles in wastewater treatment.

TiO_2 nanoparticles inevitably go through surface transformation processes both when they are used and when released into the environment. These transformations can occur when particles are exposed to UV and visible light, natural organic matter, other colloids, and solutions with varying ionic strengths.[3] Fate and transport studies that do not account for particles with environmentally transformed surfaces likely neglect a large class of materials that persist in the environment today. For example, the batch adsorption to biomass study mentioned did not address changes to the particles' surface properties that are likely to occur after environmental release. To develop a more complete understanding of the fate, transport and toxicity of TiO_2 nanoparticles, one must consider the expected variation in surface properties that result from environmental transformations.

Since many applications of TiO_2 nanoparticles involve exposure to UV irradiation,[4] it is important to study how UV exposure changes surface properties that may affect their environmental fate, transport and toxicity. Previous studies have demonstrated that exposure to UV irradiation can induce and increase the toxicity of engineered TiO_2 nanoparticles and affect their surface properties in natural waters; however, there is limited research concerning the effects of these transformations on nanoparticle fate and transport.[45, 53] This study intends to observe the effects of UV irradiation on TiO_2 nanoparticles and how that exposure affects their biosorption in wastewater treatment.

1.1 Objectives

The overarching objective of this project was to observe how exposure to UV irradiation affects TiO_2 nanoparticle biosorption to heterotrophic biomass in wastewater treatment using TiO_2 nanoparticles that have been labeled with a gold core ($Au@TiO_2$ nanoparticles). Specific objectives include the following:

1. Determining the detection limits of $Au@TiO_2$ nanoparticles in return activated sludge using instrumental neutron activation analysis (INAA).
2. Observing how exposure to UV irradiation changes the surface properties of $Au@TiO_2$ nanoparticles; specifically, particle hydrophobicity and zeta potential.
3. Observing how exposure to UV irradiation affects biosorption of $Au@TiO_2$ nanoparticles to heterotrophic biomass from a wastewater treatment plant, and correlating that behavior with observed changes in surface properties.

1.2 Hypotheses

The following are the expected results for each of the respective objectives stated above:

1. INAA can be used to detect of small quantities of labeled TiO_2 nanoparticles in ‘dirty’ matrices with high levels of background Ti, such as return activated sludge.
2. Exposure to UV irradiation will decrease TiO_2 nanoparticle hydrophobicity and decrease zeta potential.
3. Exposure to UV irradiation will influence biosorption of $Au@TiO_2$ nanoparticles to heterotrophic biomass. Any differences will be related to the hypothesized changes in TiO_2 surface properties resulting from UV irradiation.

1.3 Approach

Each objective was achieved by using Au@TiO_2 core shell particles developed by Deline et al.[63] The Au core will serve as a label to distinguish between background Ti and experimentally added TiO_2 nanoparticles. By using the known Au:Ti ratio in the synthesized particles, the amount of experimentally added TiO_2 nanoparticles can be determined by measuring the Au concentration in a sample. The approach used to accomplish each specific objective is outlined below.

1. Various concentrations of synthesized and purchased Au nanoparticles were added to return activated sludge solutions and analyzed for total Au mass using INAA to determine the detection limits of the method.
2. The effects of exposure to UV irradiation were determined by exposing synthesized particles to various sources of UV irradiation and then measuring the particles' zeta potential, hydrophobicity, and particle aggregation state. The results were then compared to the properties of particles that were not exposed to UV irradiation.
3. The impact of exposure to UV irradiation was determined by conducting batch adsorption tests to observe how exposure to UV irradiation affects biosorption of TiO_2 nanoparticles to heterotrophic biomass. Biosorption was determined by measuring the concentration of Au remaining in the supernatant using inductively coupled plasma-optical emissions spectroscopy and the mass of Au in the settled biomass using INAA. Measuring Au content in both the supernatant and the settled biomass will allow a material balance to be conducted, giving greater clarity to the results. TiO_2 concentrations were calculated from the measured Au concentrations using the Au:Ti ratio of the labeled particles.

The remainder of this thesis is organized as follows. Chapter 2 reviews literature detailing previous work related to TiO_2 nanoparticle toxicity, surface properties, and fate and transport in the environment. Chapter 3 contains a description of instruments, materials, methods, and analytical techniques used. Chapter 4 outlines and discusses the results obtained. Chapter 5 presents conclusions and suggestions for future work. Chapter 6 contains the references cited in this thesis.

2 Background

2.1 TiO_2 nanoparticle prevalence and toxicity

The production of TiO_2 nanoparticles is increasing rapidly due to their applications in a variety of products. Modeling studies predict that production rates of TiO_2 nanoparticles will reach 2.5 million tons per year by 2025. Current industry trends suggest an increased usage of nano-TiO_2 and a reduction in commonly used larger sized particles.[5]

TiO_2 nanoparticles are added to materials due to their photocatalytic activity, UV irradiation absorbing properties, and white color. Exposure of TiO_2 nanoparticles to UV irradiation generates reactive oxygen species, which can completely mineralize various recalcitrant pollutants. This creates many water treatment, antimicrobial and pollutant degradation applications, and is a primary mechanism of TiO_2 nanoparticles' toxicity to aquatic organisms.[6] Other products that utilize the properties of TiO_2 nanoparticles include sunscreens, self-cleaning materials, glare reducing coatings, paint pigments, textiles and cosmetics.[7] Additionally, TiO_2 nanoparticles are a common additive as a pigment in a variety of foods.[8]

The additions of TiO_2 nanoparticles to many different products causes the particles' release into many different environmental matrices during their production, transport, use and disposal. For many applications of TiO_2 nanoparticles, there are not established disposal procedures and methods; therefore, nanoparticles often end up being released into the environment. An example of this is the Old Danube Lake in Vienna, Austria, which is heavily used for recreational activities such as swimming during the summer. A low concentration of engineered TiO_2 nanoparticles originating from the sunscreen of beach visitors was found in the water body near popular recreation areas.[9] A study of sunscreen pollutants released into seawater by Tovar-Sanchez et al. detected TiO_2 nanoparticles originating from sunscreens offshore in southern Spain at concentrations ranging from 6.9-37.6 µg/L.[10] Other products containing TiO_2 nanoparticles that result in their release into the environment include paints and pigments. TiO_2 nanoparticles have been traced from paints on the exterior of buildings to surface water and eventually natural water bodies. The TiO_2 concentrations measured in waterbodies near the buildings were 3.5×10^7 particles/L.[11] This widespread release into the environment creates the need to understand how TiO_2 particles are transported through the environment.

Once released into the environment, TiO_2 nanoparticles are chemically stable, which reduces natural degradation and leads to accumulation. For example, models that compared nano-sized engineered TiO_2, ZnO, Ag and Carbon nanontubes found that TiO_2 is the most significant material concerning exposure due to its widespread release and

chemical stability in the environment.[12] A study of TiO_2 nanoparticles in the Rhine river found TiO_2 nanoparticles in the ng/L range in water, and mg/kg range in river sediment. In addition, nanoparticles were able to be transported downstream.[13] Due to their chemical stability, studies on environmental fate and transport of TiO_2 nanoparticles are often focused on aggregation state.[14]

TiO_2 nanoparticles in the environment pose a problem due to known toxicity to many organisms. For example, in marine environments the presence of TiO_2 nanoparticles caused hatching inhibition and malformations in *Haliotis diversicolor supertexta* (abalone) and enhanced the toxicity of tributyltin, a toxic antifouling compound, 20 fold.[15] TiO_2 nanoparticles have been demonstrated to be directly toxic to several individual aquatic species. For example, one study found that exposure to TiO_2 nanoparticles and the eventual accumulation in *Artemia salina*, (a shrimp) caused a mortality rate of 14%.[16] TiO_2 nanoparticles have also been found to be toxic to denitrifying organisms in wastewater treatment plants. Zheng et al. found that exposure of TiO_2 nanoparticles to nitrifying bacteria for 70 days reduced nitrogen removal from 80.3% to 24.4%. The long-term presence of nanoparticle reduces the microbial diversity in the activated sludge as well.[17] While these studies demonstrate the toxicity associated with exposure to TiO_2 nanoparticles, the effects were reduced at concentrations less than 2 mg/L Ti, which is well above environmentally relevant concentrations.[15,16] While the current presence of anthropogenic TiO_2 nanoparticles is not an extreme environmental threat, the accumulation of the particles in the environment may be problematic in the future. The knowledge of TiO_2 nanoparticle toxicity to many organisms and their stability in the environment creates the demand for a better understanding of how the particles enter the environment and how trends will change in the future.

TiO_2 nanoparticles also have a limited toxicity towards humans. While TiO_2 nanoparticles consumed by humans in food and beverages have little toxic effect, inhaled particles have been shown to be retained in the lungs, causing negative health effects due to their oxidative potential. [20,18] A study of the metabolism of TiO_2 nanoparticles in mice found that, upon consumption, TiO_2 concentrates in the liver and then is slowly eliminated via excretion over time, suggesting that TiO_2 nanoparticles do not accumulate in the body.[19] The toxicity of TiO_2 nanoparticles in many different environments provides motivation for determining their fate and transport once released into the environment and their removal rates in wastewater treatment facilities.

2.2 TiO_2 nanoparticles and wastewater treatment

Through many of their applications, TiO_2 nanoparticles often end up being received by a municipal wastewater treatment facility. A study by Weir found TiO_2 nanoparticles in several different foods, specifically foods colored bright white or those with a hard shell. Some foods had high enough TiO_2 concentrations that one could

consume over 100 mg in a single serving.[20] The TiO_2 nanoparticles are eventually excreted in feces and are transported to local wastewater treatment plants. Models have predicted the sources of TiO_2 nanoparticles entering a wastewater treatment facility. A model of the flow of TiO_2 nanoparticles in the Danish environment found that of all of the photostable TiO_2 nanoparticles produced (used in sunscreens, paints, foods, etc.), manufactured, and consumed, around 70% would eventually be received by a wastewater treatment facility. For photocatalytic TiO_2 (used in self-cleaning surfaces), around 35% of TiO_2 produced, manufactured, and consumed was predicted to be received by a wastewater treatment plant.[21]

Several studies have observed the concentrations of both total titanium and TiO_2 nanoparticles in various stages of municipal wastewater treatment plants. Analysis of activated sludge using single particle ICP-MS found that TiO_2 nanoparticles were in a wastewater treatment plant's influent and aeration tank at concentrations of 13.6 mg/kg and 3.3 mg/kg respectively. The same study found overall Ti concentrations in influent and aeration tanks of 3.47 mg/L and 2.15 mg/L respectively.[22] Analysis of the crystalline structure of TiO_2 nanoparticles in wastewater treatment plants by Tong et al. found that wastewater contains 30% anatase, 60% rutile and 10% ilmenite phase TiO_2, and that the phase distribution remained constant in primary treatment, secondary treatment and the effluent. The concentrations of TiO_2 in the wastewater influent was 128.9 µg/L and the dry concentration in the activated sludge was 2.4 mg/g.[23]

A different study by Kiser et al. found that for several wastewater treatment plants, 181 to 1233 µg Ti/L was found in the raw wastewater. The majority of raw wastewater Ti was larger than the 0.7 µm size fraction and was removed with 96% efficiency. Effluent concentrations were less than 25 µg/L, and the presence of both crystalline and amorphous TiO_2 nanoparticles with diameters ranging from 4-30 nm were observed. In addition, the size fractionation of titanium was conducted and found that removal of Ti that passed through a 0.7 µm glass fiber filter was <30%. [24] This shows that while the vast majority of Ti is removed by a wastewater treatment facility, removal of nano-sized TiO_2 is not as complete. This point is further demonstrated by Luo et al., who found anthropogenic TiO_2 nanoparticles accumulating on sediments in waterbodies near wastewater treatment plant effluents and then distributed throughout the aquatic environment around the discharge point.[25]

In addition to TiO_2 nanoparticles entering wastewater treatment plants through raw sewage, some have proposed intentionally adding TiO_2 nanoparticles for treatment purposes. Agbesi et al. investigated the addition of TiO_2, coated Fe_3O_4 nanoparticles to wastewater as a photo-catalyst. They found that the addition of the core-shell particles increased the photocatalytic reduction of phosphate and nitrate.[26] While the magnetic core allowed for the recovery and reuse of the particles, incomplete recovery has the potential to result in particle release in the effluent. The addition of TiO_2 to wastewater

for the purpose of enhancing treatment is still mostly experimental and is not currently a relevant source of TiO_2; however, it does represent a potential future source of TiO_2 nanoparticles in wastewater treatment.

Due to their increased production and use, TiO_2 nanoparticles have become prevalent in wastewater received by municipal treatment plant. While most Ti present in raw wastewater is removed, environmentally relevant amounts of TiO_2 nanoparticles have been found in wastewater effluents, which often discharge to surface waters. These discharges represent significant point source of TiO_2 nanoparticles into the environment. This, in conjunction with TiO_2 nanoparticles' known toxicity in aquatic system, encourages a better understanding of how particles are removed in wastewater treatment.

2.3 TiO_2 interactions with heterotrophic biomass

The term "biosorption" has been used to collectively describe several different mechanisms of associating with biomass that ultimately lead to contaminant removal in a wastewater treatment plant. For the purposes of this study, biosorption encompasses attachment to the surface of a cell, attachment to extracellular substances, and cellular uptake. While batch adsorption tests can be conducted to predict nanoparticle removal in wastewater treatment, it is important to note that any distribution isotherms or partitioning coefficients obtained are not indicative of the underlying mass transfer processes. Nanoparticle suspensions never reach thermodynamic equilibrium because they do not dissolve and therefore lack the energy input to diffuse into another phase. Therefore, the results of a batch adsorption test will only describe the macroscopic behavior of the suspension.[27]

It is the surface of the heterotrophic cells and any extracellular substances that determine the sorption of contaminants.[28] The specific mechanism associated with the attachment of a nanoparticle to bacterial surfaces or extracellular surfaces is not well understood; however, it is known that attractive electrostatic forces influence the mechanism. Thill et al. observed that nanomaterials with a positive charge exhibited strong electrostatic attraction to bacteria. [29] However, particles with a charge close to zero (both positive and negative) no longer experience normal electrostatic forces, which are repulsive. The reduced repulsive forces allow smaller attractive forces that are normally less significant to cause particle aggregation and removal from solutions.[30] Patil et al. investigated how changes in zeta potential affect the adsorption of CeO_2 nanoparticles to proteins. The study found that CeO_2 nanoparticles with a higher (more positive) zeta potential favored adsorption to proteins. This was attributed to attractive forces between the negative charged proteins and the positive charged nanoparticles.[31] It follows that changes to a nanomaterial's surface that affect the surface charge of the particle are likely to influence the biosorption of the particle to heterotrophic biomass.

The process of nanoparticles attaching to heterotrophic biomass has been previously observed. Limbach et al. observed the removal of cerium oxide (CeO_2) nanoparticles in simulated wastewater treatment and concluded through SEM imaging that attachment of CeO_2 was limited to the surface of the heterotrophic bacteria, as no nanoparticles were found within the bacteria.[32] Additional studies observing the biosorption of ZnO nanoparticles, SiO_2 nanoparticles and TiO_2 nanoparticles have been conducted by Chauque et al. and Kiser et al.; these studies modeled attachment behavior using adsorption isotherms. [33] [34] [35] The studies that have observed the behavior of metal oxide nanoparticles did not emphasize changes in particle surface properties during production, use, disposal, and release into the environment.

The biosorption of TiO_2 nanoparticles to heterotrophic biomass has been investigated. Kiser et al. applied existing batch adsorption methods to quantify TiO_2 nanoparticle biosorption to heterotrophic biomass and modeled the results with a Freundlich isotherm (R^2 value of 0.90). The same study found that at a TSS concentration of 500 mg/L, TiO_2 removal efficiency was slightly greater than 20%.[54] This study provided valuable information concerning the removal of TiO_2 nanoparticles in wastewater treatment; however, it only used a single, pristine TiO_2 source (anatase Sigma-Aldrich TiO_2 in powder form). The work can be expanded to encompass particles with different surface coatings or that have undergone surface transformations prior to being received by a treatment facility.

2.4 Impact of surface properties on TiO_2 nanoparticle fate and transport

The variety of applications for engineered nanomaterials causes their incorporation into many different products; this results in the release of engineered nanomaterials into the environment throughout the entire lifecycle of those products. As engineered nanomaterials are exposed to different environmental conditions, the particles' surface properties may be transformed. Examples include changes to a particle's zeta potential, hydrophobicity, aggregation state and steric stability. Nanoparticle surface properties are influenced by many environmental conditions including exposure to organic matter, other colloids, sunlight and solutions of varying pH and ionic strength. One of the greatest challenges in modeling the fate and transport of metal oxide nanoparticles is that even if a particle's surface properties are well understood, they can easily be transformed in environmental systems. The various interactions, transformations and reactions for metal oxide nanoparticles in the environment include coating, flocculation, agglomeration, dissolution and weathering, and adsorption of dissolved species.[36]

The fate and transport impacts of interaction with natural organic matter have been observed. Domingos et al. observed the effects of exposing TiO_2 nanoparticles to Suwannee River Fulvic Acid, and found that the particles were generally sterically

stabilized by adsorption of the fulvic acid macromolecules. This stabilization suggests that when released in the environment, exposure to natural organic matter improves particle stability, which results in greater mobility than what is predicted using unaltered nanoparticle properties.[37]

There have also been studies on how TiO_2 nanoparticle surface properties change in different water bodies. Keller et al. observed TiO_2 nanoparticles after dispersion in seawater, lagoons, rivers, groundwater and stormwater runoff and found that surface charge was most influenced by the presence of natural organic matter, ionic strength and pH. They found that electrophoretic mobility, used to determine zeta potential, was largely controlled by natural organic matter as the surface was eventually coated with organic matter, which determined the overall charge. As the total organic carbon content of the water increased, the nanoparticle charge became more negative. This has a stabilizing effect as it significantly reduced aggregation. As ionic strength increased, the TiO_2 nanoparticle charge is made more neutral, which enhances aggregation and increases removal from solution by sedimentation. pH, however, had less impact on electrophoretic mobility. Particle aggregation and removal by sedimentation was greatest in seawater, river water, and then groundwater.[38] A different study of TiO_2 nanoparticles in solutions with ionic strength and pH ranges typical of natural soils found that TiO_2 nanoparticles tend to aggregate into clusters ranging from hundreds of nanometers to several micrometers, and divalent cations such as $CaCl_2$ enhance particle aggregation.[39] These studies indicate that exposure in the environment to natural organic matter or solutions with significant ionic strengths will affect the particles' ultimate fate and transport.

Studies have also been conducted to observe how induced changes in nanoparticle surface properties designed to enhance particle efficacy in specific products impact the environmental fate and transport of the modified particles. Nonionic and anionic surfactants (Triton X-100 and ATLAS G-3300) that are commonly used as coatings to keep TiO_2 nanoparticles well dispersed when used in paints or ceramics were studied by Tkachenko et al. Both surfactants were found to enhance particle stability in natural waters, with anionic surfactants being better stabilizers.[40] This has also been investigated in natural environments. The effects of surfactants on TiO_2 nanoparticle mobility in natural soils was studied by Sun et al. and they found that surfactants decreased particle mobility in soil columns. The decreased mobility was caused by the surfactants adsorbing to both TiO_2 nanoparticles and the soils, making it an intermediary for the adsorption of TiO_2 to soil. Sun et al. hypothesized that the hydrophobic groups of the surfactants orienting towards the solution, and the hydrophilic groups being absorbed to the surface of the TiO_2 nanoparticle and soil forming a bilayer.[41] In the absence of surfactants, however, TiO_2 nanoparticles have been shown to remain suspended and readily pass

through soil columns. [42] This demonstrates that anthropogenic changes to TiO_2 nanoparticle surface properties can impact environmental fate and transport.

2.5 Effects of exposure to UV irradiation on TiO_2 nanoparticle toxicity, fate and transport

Throughout the lifecycle of products that incorporate TiO_2 nanoparticles, such as sunscreens, cosmetics or paints, it is expected that the particles will be exposed to UV irradiation. Therefore, it is important to understand how exposure to UV irradiation influences various TiO_2 nanoparticle surface properties, which ultimately dictates their toxicity, environmental fate, and transport.

Exposure of TiO_2 nanoparticles to UV irradiation has been shown to increase toxicity induced by the generation of reactive oxygen species. Studies have demonstrated that phytoplankton exposed concurrently to TiO_2 nanoparticles and natural levels of UV irradiation experienced a significant toxic response at nanoparticle concentrations that normally exhibit a low toxicity. The same study also found that concurrent exposure of TiO_2 to UV irradiation has also increased background reactive oxygen species concentrations in marine environments, which adds additional stress to ecosystems that are already impacted by thermal stress associated with global climate change.[43] A different study found that exposure of pre-UV irradiated TiO_2 nanoparticles, when compared to pre-irradiation with visible light, had no effect on the growth rates of *P. subcapitata*; rather, particle concentration most affected toxicity. This is due to the TiO_2's ability to absorb a small part of the visible light near the UV range.[44] Additionally, some species of benthic organisms, when exposed to pre-UV irradiated TiO_2 nanoparticles, experienced increased mortality rates compared to those exposed to particles not UV irradiated.[45] *Gammarus fossarum*, a leaf shredding amphipod, experienced greater adverse effects when exposed to pre-UV irradiated TiO_2 nanoparticles. UV irradiation increased ecotoxicity due to the formation of reactive oxygen species.[46] While these examples do not demonstrate that exposure of TiO_2 nanoparticles to UV irradiation dramatically increases their toxicity towards aquatic organisms, they do demonstrate smaller changes that stress the importance of considering UV irradiation exposure when conducting toxicity studies.

These toxicity studies are only relevant if there is sufficient exposure to TiO_2 nanoparticles in the environment, which is determined by the particle's surface properties. Therefore, it is important to understand how UV irradiation affects the surface chemistry of TiO_2 nanoparticles. The hydrophobicity of nanoparticle surfaces influence their fate and transport in the environment. Engineered nanoparticles with a hydrophobic surface generally aggregate and are removed from solution through sedimentation, whereas nanoparticles with a hydrophilic surface are more easily dispersed and transported through solutions.[47]

The surface of TiO_2 nanoparticles is slightly hydrophilic. Ti atoms on the surface of the nanoparticle exist predominately in 5-fold coordination (undercoordinated) and 6-fold coordination (saturated coordination). 5-fold coordinated Ti preferentially adsorbs dissociated water due to the increased presence of defects that contain Ti^{3+} sites, which leads to the formation of hydrophilic hydroxyl groups. The 6-fold coordinated Ti is generally oleophilic. The composition of the surface Ti atoms varies with nanoparticle size, which results in the hydrophilicity of TiO_2 nanoparticles being relatively greater for particles less than 6 nm in diameter.[48, 49] Exposure of the particles to UV irradiation has been shown to decrease the particles' hydrophobicity. There are multiple explanations for this phenomenon. One is that UV irradiation creates oxygen vacancies and reduces 5-fold coordinated Ti from Ti^{4+} to the Ti^{3+} state. This allows water molecules to occupy the vacancy and then dissociate creating additional hydroxyl groups on the exterior of the molecule, enhancing hydrophilicity. The majority of the hydroxyl groups bridge two Ti atoms, whereas only a small portion are terminal hydroxyl groups that bond with only one Ti atom. This is significant because bridging hydroxyl groups are acidic with a pKa of 2.9, whereas terminal hydroxyl groups are more basic with a pKa of 12.7.[52] Another explanation is that there is always a thin hydrophobic hydrocarbon monolayer on the surface of the particle due to trace amounts in the atmosphere. When this trace layer is exposed to UV irradiation, it photo-oxidizes and is removed. Both of these mechanisms result in the particle becoming more hydrophilic.[50] Wang et al. observed a contact angle of 72º on TiO_2 surfaces prior to irradiation and angles of 0-1º after irradiation for a rutile TiO_2 (1 1 0) single crystal.[51]

These changes to a TiO_2 nanoparticles' surface will affect other properties of the particle, such as hydrophobicity and surface charge. Assuming the first mechanism discussed, the replacing of surface oxygen on the exterior of the particle with acidic bridging hydroxyl groups (pKa of 2.9) would cause the electrophoretic mobility to become more negative. This was observed by Sun et. al who found that increased exposure of TiO_2 to UV irradiation shifted the electrophoretic mobility versus pH curve to the left. The isoelectric point of TiO_2 decreased from 7.0 to 6.4 after irradiation, causing an increase in particle aggregation rates at the suspension's ambient pH.[52] Wang et al. performed a similar study and also found that TiO_2 nanoparticles exposed to UV irradiation experienced increased aggregation rates; however, the presence of humic acid in the suspension improved nanoparticle stability due to increased electrostatic repulsion between particles.[53] The studies above were conducted on 80% anatase and 20% rutile TiO_2 nanoparticles without surface coatings. The results may be different for TiO_2 nanoparticles with different surface coatings or crystal structures; however, these results provide a general overview of how exposure to UV irradiation affects surface properties that influence nanoparticle attachment and aggregation. This highlights the importance of considering UV irradiation exposure when observing TiO_2 nanoparticle attachment to heterotrophic biomass.

2.6 Challenges in detecting TiO_2

Engineered TiO_2 nanoparticles are challenging to detect in complex environments. Titanium is the ninth most abundant element in the Earth's crust, and can be found in a large variety of environmental matrices.[54] The relatively high environmental background concentrations makes it challenging to distinguish anthropogenic particles from naturally occurring, nanoscale particles.[55] TiO_2 nanoparticles are commonly found in many different environments; however, current detection methods such as ICP-MS require separation methods which can be complicated for 'dirty' matrices such as activated sludge.[55] The presence of background TiO_2 can also cause complications by making it difficult to discern background Ti from TiO_2 nanoparticles added to an experiment. These challenges create the opportunity for labeled particles to assist in the study of environmental nano-TiO_2 fate. Deline et al. has demonstrated that TiO_2 nanoparticles labeled with Au cores can enhance detection in environments with significant background titanium.[63]

One method for detecting trace metals in complex matrices is instrumental neutron activation analysis (INAA). INAA is performed by bombarding samples with neutrons, resulting in the formation of radioactive isotopes. These isotopes release radioactive emissions as they decay, which can be detected using gamma ray spectroscopy. Since individual isotopes emit gamma rays with unique energies, the mass of individual elements within the sample can be determined.[56] The detection limits can be in the low parts per billion range making it a useful tool for the detection of trace metals in the environment. The use of INAA is beneficial in 'dirty' matrices as there is no separation or digestion required to prepare samples.[57] INAA analysis does render samples radioactive, making material reuse impossible. Elemental Au has a detection limit of 10-100 picograms making the use of Au labeled TiO_2 nanoparticles in complex matrices with high background Ti advantageous.[58] A study of metal concentrations in an Arizona wastewater treatment plant found that the Au concentration in return activated sludge was 177 µg/dry kg, whereas the Ti concentration was 938,820 ug/dry kg.[59] While Ti has been detected using INAA, the short half-life of its radioisotope and potential for interference with calcium (which is present in very large quantities in wastewater) make Au a better choice to analyze in wastewater. This study demonstrates the utility of using INAA to detect Au labeled TiO_2 nanoparticles for detecting anthropogenic nano-TiO_2 in wastewater samples.

Using INAA, Harper et al. has successfully characterized the uptake of gold nanoparticles in individual embryonic zebrafish assays.[60] INAA has also been used to determine the biodistribution of nanoscale gold in the individual organs of mice. A detection limit as low as 2.5 ng was obtained which corresponded to <5 ppb in the mice organs.[61] INAA has also been used to identify trace metals in activated sludge.

Specifically, McBride et al. used INAA to analyze land applied municipal sewage sludge for heavy metals. Metals such as Cd, P, Cu, Zn, and Ca were analyzed and detection was comparable to detection using ICP. However, elements that reside in mineral lattice structures were detected in greater quantities using INAA due to difficulties acid digesting the elements when preparing for ICP.[62]

This study uses Au core labeled TiO_2 nanoparticles developed by Deline et al. to distinguish from background TiO_2.[63] INAA and ICP-OES were both be used to determine Au concentrations in samples, which were then be used to quantify anthropogenic nano-Ti concentrations in sludge matrices with high background Ti.

3 Materials and Methods

3.1 Synthesis of Au@TiO_2 nanoparticles

TiO_2 coated Au nanoparticles were synthesized using a method established by Deline et al.[63] Briefly, 3-5 nm gold seed particles were synthesized by reducing gold (III) chloride trihydrate with sodium borohydride. The seeds were then grown to 30 nm gold core nanoparticles with polyvinylpyrrolidone (PVP) as a capping agent. The gold cores were then washed and rinsed by boiling in dialysis tubing, and then concentrated via centrifugation. The concentrated gold cores were then coated with TiO_2 using a hydrolysis reaction by slowly adding titanium tetraisopropoxide, and then stabilizing the particles with PVP. The coated particles were washed and rinsed using centrifugation, and then hydrothermally treated to form an anatase TiO_2 shell.

3.2 Nanoparticle Characterization

3.2.1 Metals concentration

The Au and Ti content of the Au@TiO_2 nanoparticles were measured using inductively coupled plasma optical emission spectroscopy (ICP-OES) (Spectro Arcos MultiView). Samples were digested prior to analysis using a method adapted from Goebl et. al.[64] Samples were first dewatered on a hot plate in Cole-Parmer heatable PTFE beakers at 250ºC. 1 mL of HNO_3 (Sigma Aldrich, ACS grade) and 2 mL H_2O_2 (Sigma Aldrich, ACS grade) was added to digest organics and allowed to evaporate. 5 mL of H_2SO_4 (JT Baker, ACS grade) was added and boiled until <0.2 mL remained. 5 mL of freshly prepared aqua regia was added, and boiled until < 0.2 mL remained. The addition of aqua regia can be violent if large quantities of H_2SO_4 remain, so utilize caution. 7 mL of freshly prepared 1:4 dilution of aqua regia was added, and the solution was brought to a boil. Samples were removed from heat and allowed to sit, covered, overnight. The solutions were brought to 10 mL using freshly prepared 1:4 dilution of aqua regia, and then diluted 1:5 and stored under refrigeration prior to analysis. Samples were analyzed using BDH Aristar Plus Gold Standards (1,002 ±µg/mL) standards of 75, 100, 200, 500, 1000, and 1500 ppb.

3.2.2 Instrumental Neutron Activation Analysis

1.4 mL cylindrical polyethylene vials were labeled with an original Sharpie, rinsed thoroughly, and allowed to dry at 60 ºC for 6 hours. The initial container mass was recorded. Return activate sludge (1 mL) and nanoparticles were pipetted into the vials, and samples were heated at 60ºC until they were completely dewatered. Samples were weighed, sealed and stored in a desiccator until transport to the OSU Radiation Center.

Standard preparation and sample irradiation was performed by Dr. Leah Minc at the OSU Radiation Center using the direct comparison method. The following information was provided by Dr. Leah Minc.

Five replicates of Au standard (SpecPure AAS Au) were prepared by pipetting 10 µg of liquid standard onto filter paper placed in polyethylene vials. Standards were weighed, and then deionized water was added to the vials to distribute the standard. All vials were heat-sealed.

Samples and standards were irradiated with a nominal flux of 2.6 x 10^{12} n/cm^2/s for 14 hours while rotating. Gamma counting was conducted for 10,000 s at a distance of 10 cm using a HPGe detector (Ortect GEM-25185P, 33% efficiency). The gamma spectra were analyzed with the Canberra Industries' Genie2000® software using their standard peak-search algorithm with a focus on the 411 keV peak (Au-198 peak). The mass of Au in each sample was calculated using the equation below:

$$\frac{Activity_{sample}}{Activity_{standard}} = \frac{mass_{sample}}{mass_{standard}}$$

3.2.3 Particle Size Measurement

Particle size was measured by Dynamic Light Scattering (Brookhaven Instruments, 90 Plus Particle Size Analyzer). Particles were measured at an overall colloid concentration of 10 ppm in DDI water in polystyrene cuvettes. Measurements were made in 3 runs each lasting 1 minute. Prior to measurement, particles were sonicated for 15 minutes in an ultrasonic bath (VWR B1500A-MTH).

3.2.4 Electrophoretic mobility

Nanoparticle surface charge was determined by measuring electrophoretic mobility. The electrophoretic mobility of particles was measured on a Zeta PALS (Brookhaven Instruments) at a concentration of 10 ppm. Measurements were made in 1 mM KCl at pH values 4, 5.3, 7 and 10 ± 0.05. Electrophoretic mobility measurements consisted of 5 runs with 20 cycles/run. For particles exposed to UV irradiation, solutions were made and analyzed for electrophoretic mobility within one hour of irradiation. pH was adjusted using 0.1 M HCl and 0.1 M KOH. The isoelectric point of a suspension was determined by linear interpolation of nearest positive and negative data points.

3.2.5 Hydrophobicity

Particle hydrophobicity was measured using a Rose Bengal (RB) assay described by Doktorovova et al.[65] 20 ppm of RB dye was added to nanoparticle

suspensions with a concentration range of 10 – 100 ppm, and mixed by inverting. The final volume of each solution was 1.5 mL. Samples were incubated and agitated on a shaker table for 3 hours at 25ºC, and then nanoparticles were removed from the solution via centrifugation (14,000 rpm, 20 minutes with Eppendorf Centrifuge 5415 C). The absorbance spectrum between 400 and 700 nm was measured using a Thermo Scientific Orion AquaMate 800 UV Vis spectrophotometer, measuring absorbance every 1 nm. The maximum absorbance for RB dye occurred between 541 and 543 nm, therefore the value at 542 nm was used for calculations. Samples were run in quintuplicate. Controls containing only RB dye and DDI were prepared. A partitioning quotient (PQ) was calculated using the equation below.

$$\mathrm{PQ} = \frac{\text{Mass of RB dye bound on the particle surface}}{\text{Mass of RB dye in solution}}$$

The mass RB dye was calculated from the absorbance at 542 nm using a standard curve. The mass of RB dye bound to the particle was determined by subtracting the mass of RB dye in solution from the mass of RB dye measured in the DDI controls. The partitioning quotient was plotted against the total surface area of the nanoparticle, which was calculated using the hydrodynamic diameter of the nanoparticle. Linear trendlines were added to the plots and the slopes were calculated with linear regression analysis. The slopes were compared by comparing the calculated p-value to a significance level of 0.05. Controls containing only Au@TiO_2 nanoparticles and DDI were analyzed and concluded that nanoparticle contribution to the peak was negligible.

3.2.6 Time-Resolved Dynamic Light Scattering

Homoaggregation experiments were conducted for particles with and without UV exposure. Samples were prepared by pipetting water into polystyrene cuvettes, and then adding the nanoparticles such that the concentration was 10 ppm. The particle's initial diameter was measured, and then an appropriate amount of KCl was added. 120 measurements were taken at a 15 second interval, resulting in a 30-minute run.

3.3 Determination of detection limits of Au@TiO_2 nanoparticles in return activate sludge using instrumental neutron activation analysis

3.3.1 Sample Preparation

Return activated sludge was collected from the Corvallis Wastewater Treatment Plant, transported to the lab, and stored in a refrigerator. Sludge was added to samples by inverting the sludge container three times, and then pipetting 1 mL of sludge into the pre-washed and pre-weighed polyethylene vials. Then, 10

ng, 100 ng and 10,000 ng Au@TiO_2 nanoparticles were then added in to the sludge by pipetting. Samples containing only 1 mL of return activated sludge were prepared to determine background Au concentrations. Purchased Au nanoparticles (nanoComposix) of known concentration were also analyzed. Samples in which only DDI was added were prepared to determine the degree of contamination in sample preparation. All samples were dewatered and weighed to determine the total mass solids. Samples were prepared and analyzed in triplicate.

3.3.2 Sludge analysis

Return activated sludge was analyzed for total suspended solids and total dissolved solids using Standard Methods 2540d and 2540c respectively.[66]

3.3.3 Data analysis

The results were analyzed using a Student's *t* test with a 95 % probability level. The theoretical Au concentrations based on the amount added to solution were compared with experimentally measured Au concentrations. The amount of Au associated with the nanoparticles were determined by subtracting measured values for background Au and Au associated with sample preparation contamination.

3.4 Particle exposure to UV irradiation

Particles were irradiated using one of two light sources: a 4 Watt UVP UVL-21 compact UV lamp at a wavelength of 365 nm (UVA light) and a 4000 Watt Atlas Materials Testing Solutions' Gentex SolarConstant 4000 Single Control which represents artificial sunlight. Exposure was for three hours in polystyrene or polypropylene containers, and particles were allowed to sit for 10 minutes prior to use. Samples were irradiated at the stock concentration of 233.3 ppm.

3.5 Effects of UV Exposure on biosorption to heterotrophic biomass

3.5.1 Sludge Preparation

Sludge was collected from the Corvallis Wastewater Treatment Plant and transported to the lab on ice where it was stored under refrigeration until use. Before use in adsorption tests, sludge was washed with DDI and rinsed three times using a Beckman Coulter Allegra 21 centrifuge at 800 rcf for 10 minutes. After each washing, solids were resuspended in DDI. The pH and conductivity were adjusted to pre-washing conditions (pH = 5.54 and conductivity = 191 µS/cm) using 100 mM HCl, 100 mM NaOH and 100 mM KCl. Washed and rinsed sludge was stored under refrigeration and used within 24 hours of sampling.

Return activated sludge and the washed and rinsed sludge were analyzed for pH, conductivity, total suspended solids and total dissolved solids. The TSS of the washed and rinsed return activated sludge was used to calculate the dilution factor for the batch adsorption experiment.

3.5.2 Batch adsorption test

Batch adsorption tests were conducted in well rinsed 50 mL centrifuge tubes. Au@TiO_2 nanoparticles were sonicated in an ultrasonic bath (VWR B1500A-MTH) for 15 minutes and then either irradiated for 3 hours or left in the dark. Nanoparticles were then added to a 50 mL polypropylene centrifuge tube containing deionized water such that the final particle concentration (after the eventual addition of return activated sludge) was 3.68 ppm. Samples were prepared in triplicate.

Washed and rinsed return activated sludge was then added to the centrifuge tube such that the final concentration was 500 ppm and the final volume was 30 mL. Samples were inverted to mix, and then agitated in the dark for 3 hours. The biomass was then allowed to settle by gravity for 30 minutes. A blank which contained only biomass was prepared to determine background concentrations of gold and a control was prepared in which no biomass was added.

After settling, 10 mL of supernatant was drawn off using a pipette and stored for later digestion and ICP-OES analysis. The rest of the supernatant was then pipetted off until ~3 mL remained. Settled biomass was collecting by pipetting 1 mL into the polyethylene vials and prepared for INAA using the method described above.

4 Results

4.1 Detection Limits of Au@TiO_2 nanoparticles in return activated sludge using INAA.

Figure 1 shows the results of the INAA detection limit experiment and breaks down the total measured Au into three sources: Au from the return activated sludge, Au from contamination in the sample preparation process, and the calculated amount of Au from the added Au@TiO_2 nanoparticles. The calculations are in Appendix 6.4.

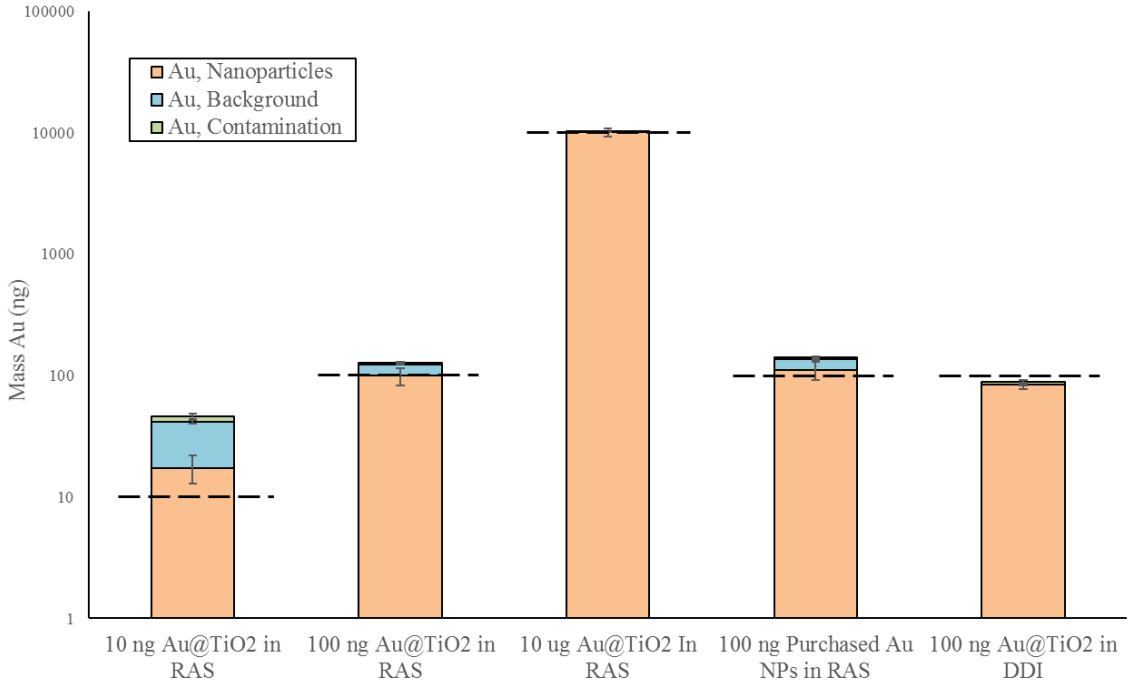

Figure 1. Mass Au measured in samples spiked with Au@TiO_2 nanoparticles and purchased Au nanoparticles. Samples were spiked in 1 mL return activated sludge or DDI . Measured Au is broken down into Au from contamination, background RAS, and added nanoparticles. Error bar represent 95% confidence intervals. Dashed lines represent the expected amount of Au associated with the added nanoparticles. Note that the y-axis is logarithmic.

Analysis of the samples that contained only 1 mL of DDI water detected an average mass Au of 4.67 ± 1.84 ng. This suggests that there may have been contamination associated with the sample preparation process. A potential source of this contamination is the INAA vial itself. Contamination of the interior or exterior of the INAA vials during sample preparation or transport may have also contributed to the detection of Au in the DDI controls.[67] Another source of the measured Au is general laboratory contamination associated with pipettes, glassware, spray bottles etc. Future analysis of INAA vials with no added material is necessary to determine if the contamination is associated with the vials (if Au is detected) or the sample preparation

process (if no Au is detected). Because the source of this contamination is uncertain, it was assumed that contamination was present in every sample and therefore identified as a source of Au in Figure 1. This contamination is very significant for the samples spiked with 10 ng Au from Au@TiO_2 nanoparticles, as it represents almost half of the added mass. The contamination is also relevant for samples spiked with 100 ng Au from Au@TiO_2 nanoparticles, however the contamination is an order of magnitude less than the added mass and therefore is less significant. For the samples containing 10 µg of Au from Au@TiO_2 nanoparticles, 4.67 ng Au is four orders of magnitude less than the expected mass, therefore the effects of contamination are negligible.

The background Au was determined by INAA of the samples that contained only 1 mL of return activated sludge. The average value of Au in the return activated sludge was 24.0 ± 1.2 ng. The TSS and TDS of the return activated sludge were 5358 ± 577 mg/L and 287 ± 50 mg/L respectively. This corresponds to an average Au content in dry return activated sludge of 4479.3 ± 532 µg/kg. A previous study of two wastewater treatment plants found Au concentrations in return activated sludge of 177 and 580 µg/dry kg;[59] the mass Au measured in return activated sludge for this study was considerably greater than values from other studies. A potential explanation for this difference is the methods used to determine concentration, as this study determined Au content using INAA whereas Westerhoff et al. used ICP-MS. In addition, the return activated sludge analyzed by Westerhoff et al. was collected in Arizona, whereas this study used wastewater from Corvallis, Oregon. The difference in the background Au concentration could be due to regional variation in surrounding industry. Using the average value, the limit of detection and the limit of quantification in 1 mL of return activated sludge was determined to be 27.8 ng and 35.5 ng, respectively. These calculations are shown in Appendix 6.4.

The background Au in returned activated sludge influenced the total amount of Au detected in samples spiked with 10 and 100 ng Au from Au@TiO_2 nanoparticles; it was less relevant for the samples spiked with 10 µg Au from Au@TiO_2 nanoparticles. In order to estimate the amount of experimental Au that was associated with the Au@TiO_2 nanoparticles, the background and contamination masses of Au were subtracted from the total Au measured in the sample. This assumes that background Au was consistent for each of the sludge samples, which cannot be verified; however, the simplification allows for a useful estimate of how much measured Au was associated with the addition of Au@TiO_2 nanoparticles.

The first bar in Figure 1 shows the total mass of Au measured using INAA in 1 mL return activated sludge samples spiked with Au@TiO_2 nanoparticles. The expected mass of Au from Au@TiO_2 nanoparticles was 10 ng, and is represented by the dashed black line. The total Au measured was 46.0 ± 2.5 ng. These results illustrate that the background Au exceeded the mass of Au associated with the added Au@TiO_2

nanoparticles. However, after accounting for background Au and contamination, the mass Au associated with Au@TiO_2 nanoparticles was 17.3 ± 4.3 ng; this value is less than the limit of quantification in 1 mL of return activated sludge of 35.5 ng. It follows that 10 ng of Au added in the form of Au@TiO_2 nanoparticles is too small to reliably measure with INAA against a background of 1 mL return activated sludge. A more detailed figure showing the calculated sources of measured Au is in Appendix 6.1.

The second bar in Figure 1 shows the breakdown of 100 ng Au from Au@TiO_2 nanoparticles in return activated sludge. The calculated mass of Au associated with the nanoparticles was 99.3 ± 16.0 ng. A hypothesis test confirms that the calculated value was not statistically different from the expected value of 100 ng (represented by the dashed line). This value can be compared with the values for 100 ng of Au from Au@TiO_2 nanoparticles added to DDI (bar 4 of Figure 1) to determine the effects of the matrix on the Au measurement. The calculated amount of Au from nanoparticles was 84.3 ± 7.0 ng, and was determined by subtracting the contamination value from the total mass Au measured. The calculated values of Au associated with Au@TiO_2 nanoparticles in DDI vs return activated sludge were not statistically different. This confirms that background Au in the return activated sludge was responsible for the higher than expected amount of Au measured. Purchased Au nanoparticles were added to return activate sludge and analyzed so that the recovery of Au@TiO_2 nanoparticles could be compared to the recovery of Au in a similar form. This could then determine if the presence of the TiO_2 shell impacted the amount of Au measured by INAA. The calculated mass of Au associated with the citrate capped Au nanoparticles was 111.3 ± 7.7 ng. This value is not statistically different from the calculated mass of Au associated with the addition of Au@TiO_2 nanoparticles in return activated sludge. See Appendix 6.1 for a more detailed Figure to compare the calculated values. These results demonstrate that INAA can be used to detect 100 ng Au from Au@TiO_2 nanoparticles in return activated sludge if the background concentration is known.

The third bar of Figure 1 shows the total Au measured in 1 mL return activated sludge; samples were spiked with Au@TiO_2 nanoparticles with an expected Au mass of 10 µg. The calculated amount of Au associated with the nanoparticles was 10,012 ± 744 ng. These results demonstrate that background Au and contamination was negligible compared to the deviation in total Au measured. Furthermore, INAA was used to accurately detect 10 µg of Au from Au@TiO_2 nanoparticles in 1 mL of return activated sludge.

Figure 1 demonstrates that INAA can be used to detect Au-labeled TiO_2 nanoparticles in dirty matrices such as return activated sludge, making these methods appropriate for evaluating the biosorption of TiO_2 to heterotrophic biomass in batch adsorption tests. The batch adsorption tests conducted to observe the effects of UV

irradiation on the biosorption of TiO_2 had an initial Au nanoparticle concentration of 1.68 ppm in 30 mL solution. Assuming a removal efficiency of 20-40%,[35] the expected mass of Au nanoparticles in the settled solids ranges from 9 to 18 µg. This is well within the range of accurate detection in return activated sludge using INAA. In addition, INAA was able to detect ng scale Au, making it a powerful tool for fate and transport analysis. These results can be improved on however. Future work should determine if the contamination associated with the sample preparation is due to the DDI water used, the INAA vials, or the materials used to prepare the solutions. In addition, additional return activated sludge samples should be analyzed to confirm the higher than expected background Au concentration.

4.2 Effects of UV irradiation on Au@TiO_2 nanoparticle surface properties

Figure 2 shows the effects of UV irradiation on Au@TiO_2 nanoparticles. For all pH values, exposure to UV irradiation decreased the electrophoretic mobility of the nanoparticles. The calculated isoelectric point for particles exposed to UVA radiation, artificial sunlight, and dark controls were 6.1, 6.0 and 7.0, respectively. A statistical hypothesis test determined that at pH 5.4, 7.0 and 10.0, there was no difference between the electrophoretic mobility of particles exposed to UVA radiation and artificial sunlight. Additional hypothesis testing concluded that the electrophoretic mobility of the dark control was statistically different from that of samples exposed to UVA radiation and artificial sunlight at every pH value tested. This suggests that the source of UV irradiation did not affect the reduction in electrophoretic mobility.

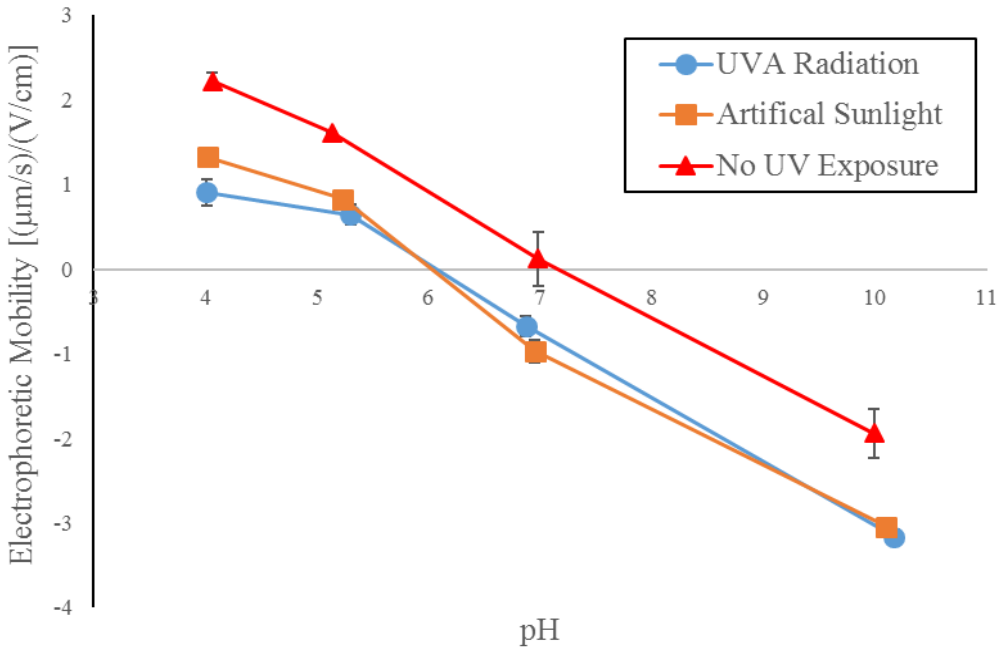

Figure 2. Electrophoretic Mobility of Au@TiO_2 nanoparticles exposed to UVA radiation, artificial sunlight, and the dark control. Error bars represent 95% confidence intervals. The calculated zeta potential of the Au@TiO_2 nanoparticles is in Figure 12 of Appendix 6.2.

These results are consistent with the findings of Sun et al., who proposed that the UV irradiation of the TiO_2 surface creates oxygen vacancies that become occupied by water, which dissociates to form hydroxyl groups. ATR-FTIR spectroscopy concluded that most of the hydroxyl groups were bridging hydroxyls (pKa of 2.9) as opposed to terminal hydroxyls (pKa of 12.7). Furthermore, the generation of additional acidic bridging hydroxyl groups contributed to shift of the electrophoretic mobility versus pH curve to the left.[52] The findings by Sun et al. were on bare TiO_2 nanoparticles, while the Au@TiO_2 nanoparticles used in this work were coated with polyvinylpyrrolidone (PVP). As such, the change in electrophoretic mobility may have been due to the photodegradation of the PVP coating. Additional characterization such as ATR=FTIR would determine if the PVP coating degraded; in addition, further testing on bare Au@TiO_2 nanoparticles would help separate the effects of the PVP coating from the effects associated with changes of the metal oxide surface itself.

The impacts of UV irradiation on Au@TiO_2 nanoparticles was also studied. The results are summarized in Figure 3, which compares the partitioning coefficient (ratio of Rose Bengal bound on the nanoparticle surface to the Rose Bengal in solution) to the total nanoparticle surface area. Therefore, a larger slope is associated with greater adsorption of Rose Bengal per unit area of nanoparticle surface; since Rose Bengal is hydrophobic, a larger slope is indicative of a more hydrophobic nanoparticle surface. Hypothesis tests comparing the slopes confirmed that each slope is statistically different

from the other two. Therefore, Figure 3 demonstrates that Au@TiO_2 nanoparticle exposure to UV irradiation caused the hydrophobicity of the surface to decrease. In addition, the artificial sunlight caused a greater decrease in the hydrophobicity of the Au@TiO_2 nanoparticles than UVA radiation.

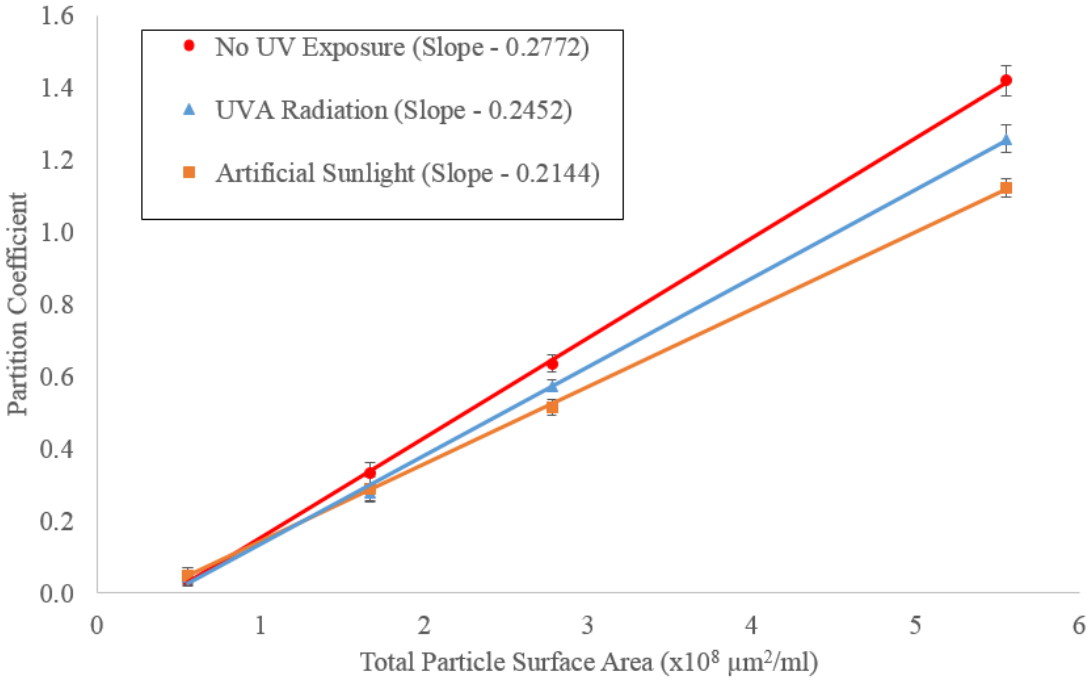

Figure 3. Relative hydrophobicity of Au@TiO_2 nanoparticles measured by adsorption of Rose Bengal dye on the nanoparticle surface. The partitioning coefficient is the ratio of Rose Bengal bound on the nanoparticle surface to the Rose Bengal in solution. The total particle surface area was calculated using a particle hydrodynamic diameter of 245.4 nm.

These results can be explained by the mechanism proposed by Sun et al. described above. The addition of hydroxyl groups on the nanoparticle surface makes it more hydrophilic.[52] The decrease in hydrophobicity could also be explained by the photodegradation of the PVP coating or other organics on surface of the nanoparticles. Additional analysis of Rose Bengal assays containing bare Au@TiO_2 nanoparticles is necessary to determine the effects of the PVP coating on nanoparticle hydrophobicity.

The Rose Bengal assay provides a rapid and facile method for comparing the relative hydrophobicities of nanomaterials. However, there are some limitations to using this method. Rose Bengal contains a charge that varies with pH, which presents the possibility of electrostatic interactions causing inaccuracies.[68] Since exposure to UV irradiation also caused changes to the electrophoretic mobility of the Au@TiO_2 nanoparticles, it is difficult to determine how much impact electrostatic forces had on the measured decrease in hydrophobicity. The assays can be expanded to include a

hydrophobic molecule that does not have a charge such as naphthane to determine the impact of electrostatic interactions.[69] In addition, this work can be expanded to include hydrophilic dyes such as Nile Blue. Using both hydrophobic and hydrophilic dyes can show the continuum of Au@TiO_2 nanoparticle surfaces from hydrophobic to hydrophilic.[69] These additional experiments should be conducted in the future to provide greater detail concerning the effects of UV irradiation of Au@TiO_2 nanoparticle hydrophobicity.

4.3 Batch adsorption test

Figure 4 illustrates the set up for the batch adsorption test before and after 30 minutes of settling. The total volume was 30 mL. The top 10 mL of supernatant was sampled and analyzed using ICP-OES and the bottom 1 mL of settled sludge was sampled and analyzed with INAA. Freshly collected, washed and rinsed return activated sludge used for the batch adsorption experiment. The TSS and TDS of the washed and rinsed return activated sludge were 8811 ± 233.3 mg/L and 371 ± 68 mg/L, respectively. INA analysis of controls containing only return activated sludge found a background Au concentration of 2,176 ± 381 µg/kg. Given an initial TSS of 500 mg/L for each solution, the initial background Au concentration was 0.033 ± 0.003 µg/L. This is negligible compared to the initial Au concentration from the added Au@TiO_2 nanoparticles of 1.68 mg/L. In addition, the expected contamination associated sample preparation (4.67 ± 1.84 ng) was also negligible.

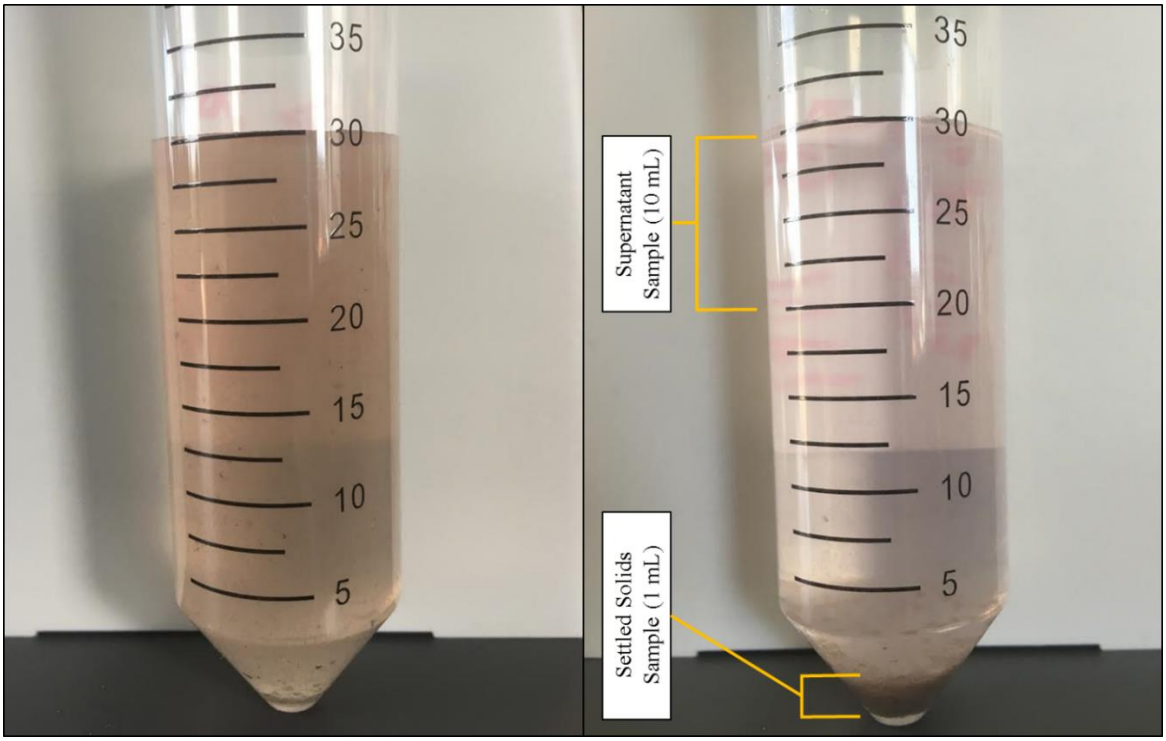

Figure 4. Image of batch adsorption test before (left) and after (right) 30 minutes of settling.

The average concentration of Au and Ti measured in the supernatant of the batch adsorption test for particles exposed to UVA radiation, artificial sunlight, and the dark control are shown in Figure 5. The concentration was measured using ICP-OES and the Au:Ti ratio of the synthesized Au@TiO_2 nanoparticles was 1:1.29. The average background Ti concentration of the return activated sludge was 0.37 ± 0.58 ppm. In Figure 5 the Ti associated with the Au@TiO_2 nanoparticles was determined by subtracting the background Ti concentration from the total Ti concentration measured. This indicates that Ti concentrations were significantly lower than expected. Figure 13 in Appendix 6.3 shows calculated Ti associated with Au@TiO_2 nanoparticles compared to the expected values. This difference in expected and measured Ti concentrations may be associated with low recovery of Ti in the digestions. The use of controls containing known amounts of TiO_2 nanoparticles digested in parallel with supernatant samples could be used in the future to help determine the source of the poor recovery.

Hypothesis testing concluded that none of the measured Ti concentrations were statistically different from one another; however, the measured Au concentrations for UVA radiation and artificial sunlight were statistically different from the dark controls. The high amount of variation of measured Ti across samples containing return activated sludge demonstrates the utility of using Au cores as a label for TiO_2 nanoparticles in matrices containing background Ti. Therefore, for all samples the removal efficiency of Au@TiO_2 nanoparticles was determined solely using measured Au concentrations.

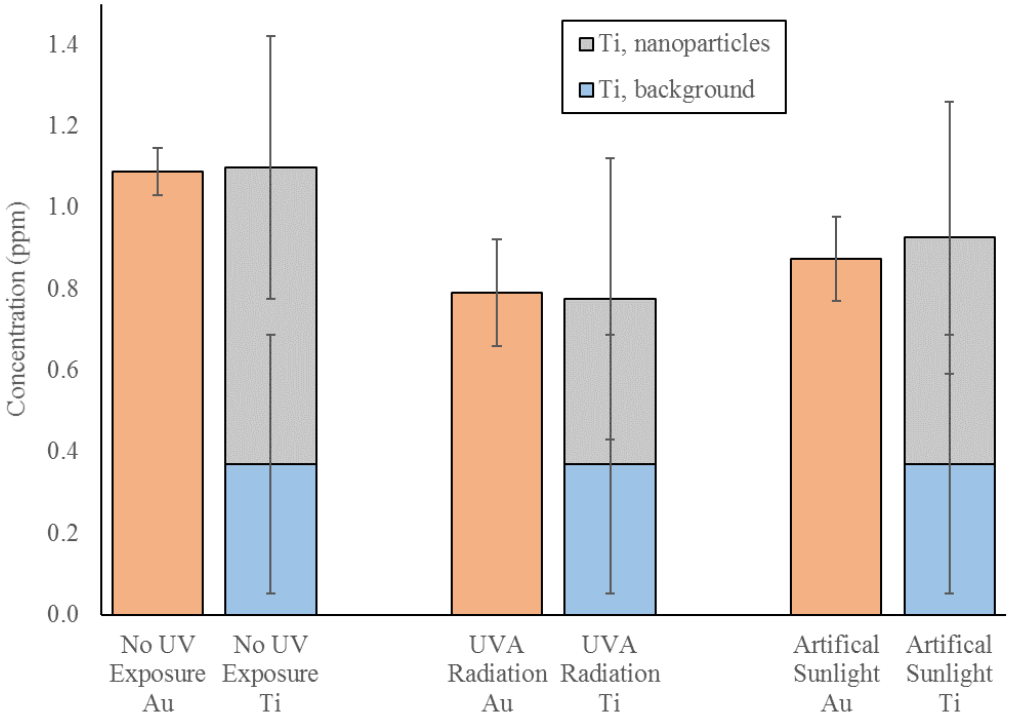

Figure 5. Average concentrations of Au and Ti measured in supernatant of batch adsorption test. Samples were run in triplicate. Error bars represent 95% confidence intervals.

Figure 6 shows the results of a material balance identifying the fate of Au in the batch adsorption tests. The mass of Au in the supernatant was determined by assuming the concentration (measured using ICP-OES) in the 10 mL samples was consistent throughout the entire 29 mL of supernatant. The mass of Au in the settled solids was the total mass measured by INAA in the bottom 1 mL of the solution. These values were added together, and compared to an expected total mass Au of 54.0 ng which is represented by the dashed line. The total expected mass was based on the known amount of Au added as Au@TiO_2 nanoparticles. Hypothesis testing concluded that the expected mass of Au was statistically different from the combined mass for the dark controls and particles exposed to artificial sunlight; however, the total mass of particles exposed to UVA irradiation was not statistically different from the expected mass.

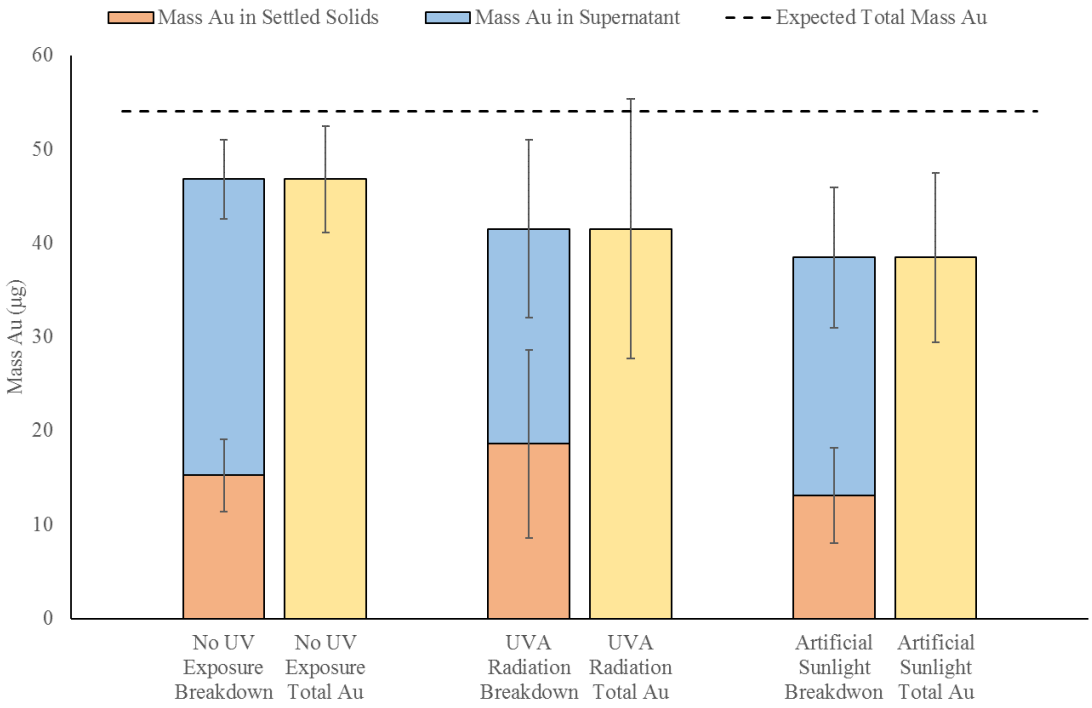

Figure 6. Material balance of Au measured in supernatant and Au measured in settled solids. Error bars represent the 95% confidence intervals of the combined mass.

The material balance in Figure 6 indicates that not all of the Au was accounted for in the batch adsorption test. Specifically, the percent recovery for the dark controls, samples exposed to UVA radiation and artificial sunlight was 86.6 ± 10.5%, 76.9 ± 25.6%, and 71.2 ± 16.7%, respectively. One possible explanation for the incomplete Au recovery is Au or biomass attaching to the surface of the polypropylene centrifuge tubes used for the adsorption test. Another explanation for the low recovery of Au in the supernatant is an incomplete nanoparticle digestion. The magnitude of losses during the digestion process can be determined by digestion controls with known concentrations of Au nanoparticles in parallel to the standard digestion. Low Au recoveries for the control

would indicate low recoveries in the supernatant samples. Another explanation for the low Au recovery is inconsistent Au concentrations across the supernatant. The material balance in Figure 6 assumes that the supernatant concentration is constant throughout the solution. This possibility can be assessed by either taking a larger, more representative supernatant sample, or by taking additional samples and observing if the Au concentration changes throughout the supernatant.

The Au measured in the 1 mL of settled solids has two potential sources: Au@TiO_2 nanoparticles free in the solution and Au@TiO_2 nanoparticles that are associated with biomass and settled to the bottom of the solution. Figure 14 in Appendix 6.3 shows the calculated breakdown of Au NP sources in the 1 mL of settled solids. In the settled solids, the Au associated with the solution is considerably less than the amount associated with the biomass. The concentration of free Au@TiO_2 nanoparticles was assumed to be equal to the concentration measured in the supernatant. This assumes that settling was not a major mechanism for nanoparticle removal. A similar study by Kiser et al. suggested that the biosorption of nanomaterials to biosolids is the predominant mechanism for removal.[54] However, if the Au@TiO_2 nanoparticles homoaggregated in the return activated sludge solution, settling may have been a more relevant removal mechanism. In addition, nanoparticle aggregation is affected by the solution's ionic strength, suggesting that Au@TiO_2 nanoparticle aggregation may have occurred. Therefore, time-resolved dynamic light scattering was conducted on Au@TiO_2 nanoparticles in solutions of filtered (0.2 µm nylon) return activated sludge to determine whether homoaggregation was present. The results of the TR-DLS analysis are in Figure 7, and indicate that Au@TiO_2 nanoparticle diameter did not change significantly in the filtered return activated sludge.

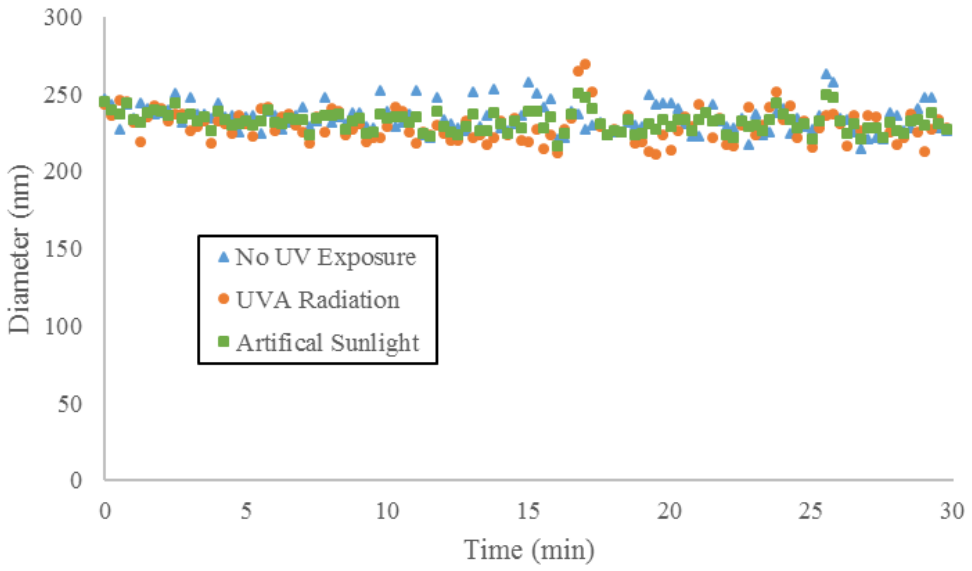

Figure 7. Homoaggregation of Au@TiO_2 nanoparticles in filtered return activated sludge.

The terminal settling velocity of a 245 nm nanoparticle, calculated using Stokes' law, is 4.96 x 10^{-8} m/s. This is extremely slow, as it would require 2.33 days for a particle to settle 1 cm. This suggests that homoaggregation and then sedimentation was not a relevant mechanism of the removal of Au@TiO_2 nanoparticles. However, additional analysis of controls could verify if settling was a relevant removal mechanism. Specifically, Au@TiO_2 nanoparticles could be added to return activated sludge supernatant. After 30 minutes of settling, analysis of the supernatant and the bottom 1 mL would indicate whether significant particle settling occurred.

Analysis of the amount of Au in the supernatant compared to the settled solids can be used to determine the biosorption of TiO_2 nanoparticles to heterotrophic biomass. In the similar study by Kiser et al., an increase in nanoparticle removal from the supernatant was used to indicate an increase in biosorption to heterotrophic biomass. This is because biosorbed nanoparticles are removed when the biomass settles out of solution. [54]

The percent removal of Au@TiO_2 nanoparticles can be determined using either the supernatant data or the settled solids data.

The percent removal of Au@TiO_2 nanoparticles was calculated using the concentration of Au in the supernatant with the equation below. The initial Au concentration of Au was 1.68 mg/L. This determination of removal is consistent with the calculation by Kiser et al. in a similar study.[54]

$$\text{Percent Removal} = \frac{\text{initial Au concentration-concentration Au in supernatant}}{\text{initial Au concentration}}$$

The percent removal of $Au@TiO_2$ nanoparticles was determined using the mass of Au in the settled solids with the equation below. The initial mass of Au was determined using the initial concentration of 1.68 mg/L and the overall volume of 30 mL.

$$\text{Percent Removal} = \frac{\text{mass Au in settled solids}}{\text{initial mass Au in solution}}$$

The results of the two different percent removal calculations are shown in Figure 8. Analysis of the percent removal calculated using the supernatant data shows that $Au@TiO_2$ nanoparticle removal increased with exposure to UVA radiation and artificial sunlight. A hypothesis test confirms that the percent removal for particles exposed to UVA radiation and artificial sunlight were statistically different from the percent removal of the dark controls. Using the supernatant data, the calculated percent removal for particles exposed to UVA radiation, artificial sunlight and the dark controls was 51.3%, 46.1% and 33.0% respectively. These values were similar to the values from Kiser et al., who observed ~24% removal of Ti in 400 mg/L total suspended solids of biomass.[35] Furthermore, the supernatant data indicates that exposure to UV irradiation increased the biosorption of $Au@TiO_2$ nanoparticles to heterotrophic biomass. This increase in biosorption can be compared to the expected changes associated with the decrease in electrophoretic mobility and hydrophobicity discussed in section 4.2. A decrease in hydrophobicity should cause a decrease in biosorption to heterotrophic biomass, as nanoparticles that are more hydrophilic would be more likely to remain in the liquid phase. In addition, a reduction in electrophoretic mobility should reduce biosorption to heterotrophic biomass; this is due to a decrease in attractive forces between the negatively charged biomass and the $Au@TiO_2$ nanoparticle. Further research on the effects of UV irradiation on $Au@TiO_2$ nanoparticle surface properties is necessary to explain the correlation between UV exposure and increased biosorption to heterotrophic biomass.

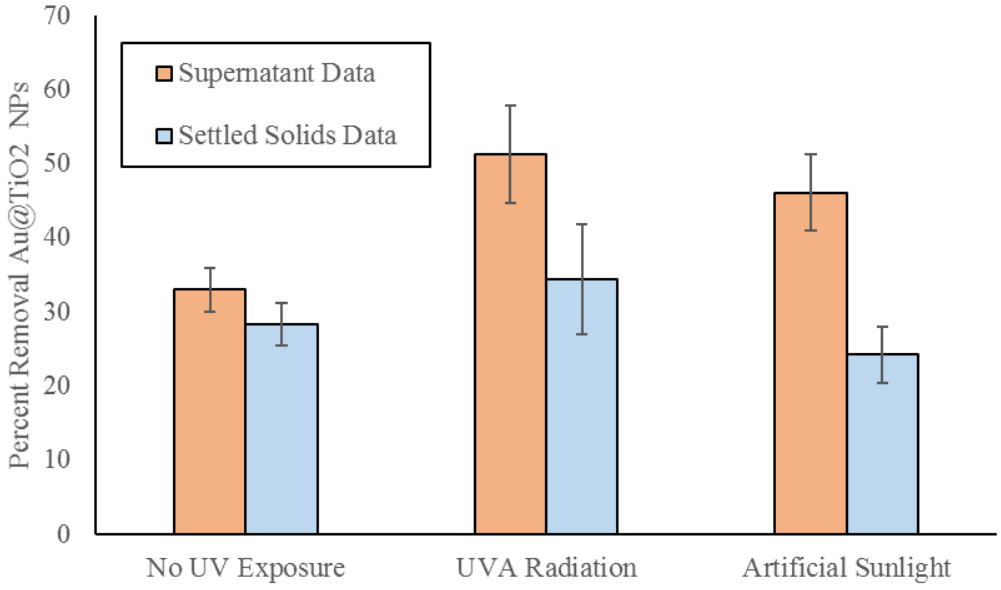

Figure 8. Comparison of the percent removal of Au@TiO_2 nanoparticles calculated using the Au concentration in the supernatant and the settled solids. Error bar represent 95% confidence intervals.

There are limitations associated with using the supernatant to determine Au@TiO_2 nanoparticle biosorption to heterotrophic biomass. After 30 minutes of settling, not all of the biomass had settled out of solution; therefore, some of the Au detected in the supernatant likely had been biosorbed to the heterotrophic biomass. Additional tests that completely remove the biomass from the solution would be necessary to obtain more accurate values for Au@TiO_2 biosorption. In addition, testing the supernatant does not account for Au@TiO_2 removal due to attachment to the vessel walls. To develop a better understanding of Au@TiO_2 nanoparticle removal efficiency, the mass of Au in the settled solids needs to be analyzed.

Analysis of the percent removal of Au@TiO_2 nanoparticles calculated using the mass Au measured in the bottom 1 mL provides a different conclusion. Percent removals calculated using the settled solids were lower than the values calculated using the supernatant. In addition, a hypothesis test concluded that there were no statistical differences between the removal of particles exposed to UVA radiation, artificial sunlight, and the dark controls. This indicates that exposure to UV irradiation did not affect Au@TiO_2 nanoparticle removal. Using the settled solids to determine percent removal from the mass Au in the settled solids also has limitations. Since the 1 mL collected sample contained unattached Au@TiO_2 nanoparticles (see Figure 14 in in Appendix 6.3), the total mass Au analyzed by INAA likely overestimated the biosorption of Au@TiO_2 nanoparticles to heterotrophic biomass. To determine a more accurate value

for the biosorption of $Au@TiO_2$ nanoparticles, the biomass must be removed from the solution prior to analysis.

Analysis of the percent removals calculated using the supernatant data and the settled solids data results in different conclusions concerning the effects of UV irradiation. Hypothesis testing confirms that for particles exposed to UVA radiation and artificial sunlight, the two methods of determining percent removal yielded statistically different values. Comparing the two methods, INA analysis of the settled solids provides a more direct measurement of percent removal than the supernatant data does. The supernatant data does not account for potential losses such as attachment to the vessel walls, whereas the settled solids data is a direct measurement of what was removed. This suggests that the settled solids data more accurately describes biosorption to heterotrophic biomass. Additional research that closes the material balance by quantifying attachment to the container walls, improving ICP-OES and INAA preparation methods, and measuring a greater portion of the supernatant is necessary to determine which method is a better indicator of biosorption to heterotrophic biomass.

5 Conclusions

5.1 Conclusions

The overall goal of this research was to determine the effects of UV irradiation on the biosorption of TiO_2 nanoparticles to heterotrophic biomass. This was achieved through three different objectives, listed in Chapter 1.2. The major findings associated with each objective are:

1) Detection Limits of Au@TiO_2 nanoparticles in return activated sludge using INAA.
   a) INAA analysis of two different samples of return activated sludge found Au contents of 2,176 ± 381 µg/kg and 4479.3 ± 532 µg/kg, both higher values than what was reported in previous studies.
   b) The limit of detection and the limit of quantification of Au@TiO_2 nanoparticles in 1 mL of return activated sludge was calculated to be 27.8 ng and 35.5 ng, respectively.
   c) Contamination associated with the INAA sample preparation was measured 4.67 ± 1.84 ng of Au.
   d) Au@TiO_2 nanoparticles can be detected using INAA in return activated sludge by measuring the total mass of Au.
   e) When performing experiments on the ppb scale, it is important to measure the background mass Au present in sludge and the mass Au associated with contamination during sample preparation. As the expected mass of Au nanoparticles increases to the ppm scale the effects of background Au and contamination become less significant.
2) Effects of UV irradiation on Au@TiO_2 nanoparticle surface properties.
   a) Exposure to UV irradiation reduced the Au@TiO_2 nanoparticle electrophoretic mobility and shifted the electrophoretic mobility vs pH curve to the left.
   b) Exposure to UV irradiation decreased the hydrophobicity of Au@TiO_2 nanoparticles.
3) Batch Adsorption test
   a) The supernatant data demonstrated higher variation in the measured Ti concentrations than the measured Au concentrations. Recovery of Ti was also less complete than expected. This emphasizes the utility of using Au nanoparticle labels to quantify experimental TiO_2 nanoparticles.
   b) Analysis of the measured Au in settled solids and the supernatant lead to an incomplete material balance. Additional analysis will be necessary to close the material balance.
   c) The data from the supernatant of the batch adsorption tests indicated that exposure to UV irradiation increased the removal of Au@TiO_2 nanoparticles

in return activated sludge. This indicates UV irradiation increases the adsorption of TiO_2 nanoparticles to heterotrophic biomass. However, the data from the settled solids did not find a relationship between UV irradiation and Au@TiO_2 nanoparticle removal.

5.2 Implications

While additional testing is necessary to characterize the biosorption of TiO_2 nanoparticles to heterotrophic biomass, the results of this study have several practical implications. The use of INAA to detect Au labeled TiO_2 nanoparticles in complex matrices was novel work and has a wide variety of fate and transport applications. The characterization of the effects of UV irradiation on TiO_2's surface properties highlights the importance of acknowledging nanoparticle surface transformations when conducting fate and transport studies. The results of this study represent a starting point for future studies on the effects of UV irradiation on TiO_2 nanoparticles that must be considered when developing regulations for the use of nanomaterials.

5.3 Future Work

The results of this study can be built upon to improve understanding of the effects of UV irradiation on the biosorption of TiO_2 nanoparticles to heterotrophic biomass. The following is list of research topics that will improve upon this work:

- Measure the Au associated with the INAA containers. This will determine if the source of the contamination is associated with the containers or the sample preparation process.
- Analyze how UV irradiation affects the surface properties of uncoated Au@TiO_2 nanoparticles. This will determine if the changes observed in this work were associated with the TiO_2 surface or the PVP coating. Use methods such as ATR-FTIR to identify changes in the PVP structure.
- Perform hydrophobicity assays using Nile Blue and naphthane. This will provide detail as to the effects of UV irradiation on Au@TiO_2's hydrophilicity and determine the impacts of electrostatic interactions.
- Digest controls containing known amounts of TiO_2 and Au nanoparticles in parallel to sample digestion. This will determine if there are significant Au or Ti losses during sample digestion prior to ICP-OES.
- Analyze a greater volume of supernatant during the batch adsorption test for comparison. This will determine if the incomplete Au material balance is associated with an inconsistent Au concentration throughout the supernatant.
- Quantify Au@TiO_2 nanoparticle removal by settling. This should be done by adding Au@TiO_2 nanoparticles to the supernatant of return activated sludge, and measuring the concentration of Au at various heights. This will determine

whether settling was a significant removal mechanism for the batch adsorption tests.

6. Appendix

6.1 Detection Limit Graphs

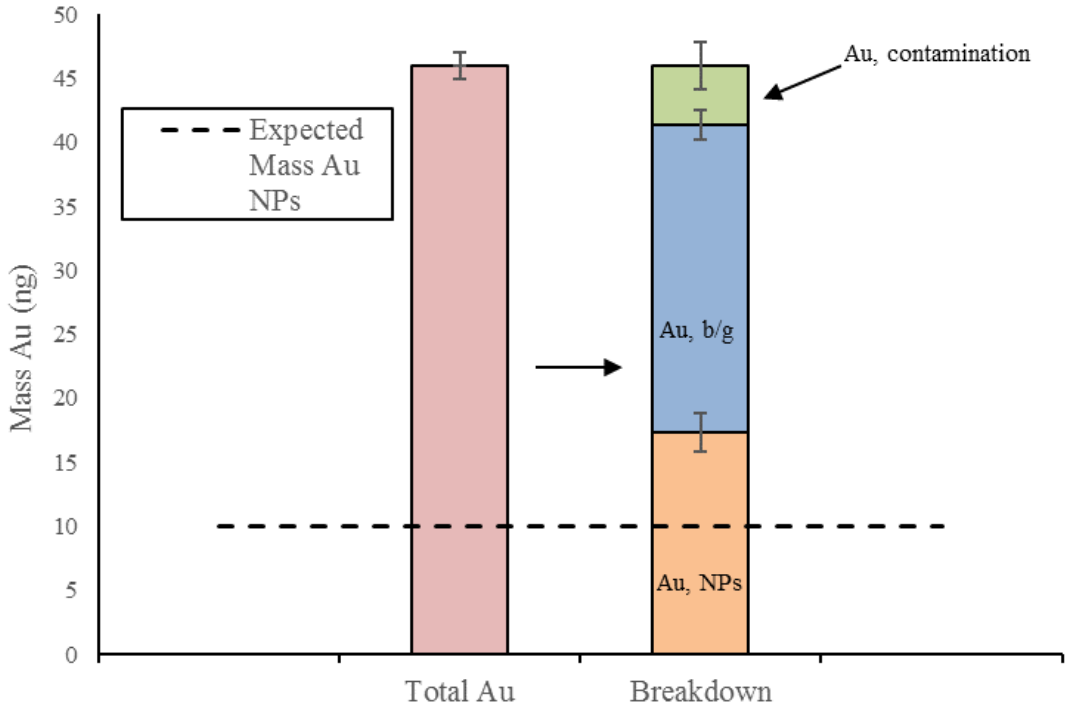

Figure 9. Mass Au measured in samples spiked with 10 ng Au from Au@TiO_2 nanoparticles in 1 mL return activated sludge, and the breakdown of Au sources. Error bar represent 95% confidence interval

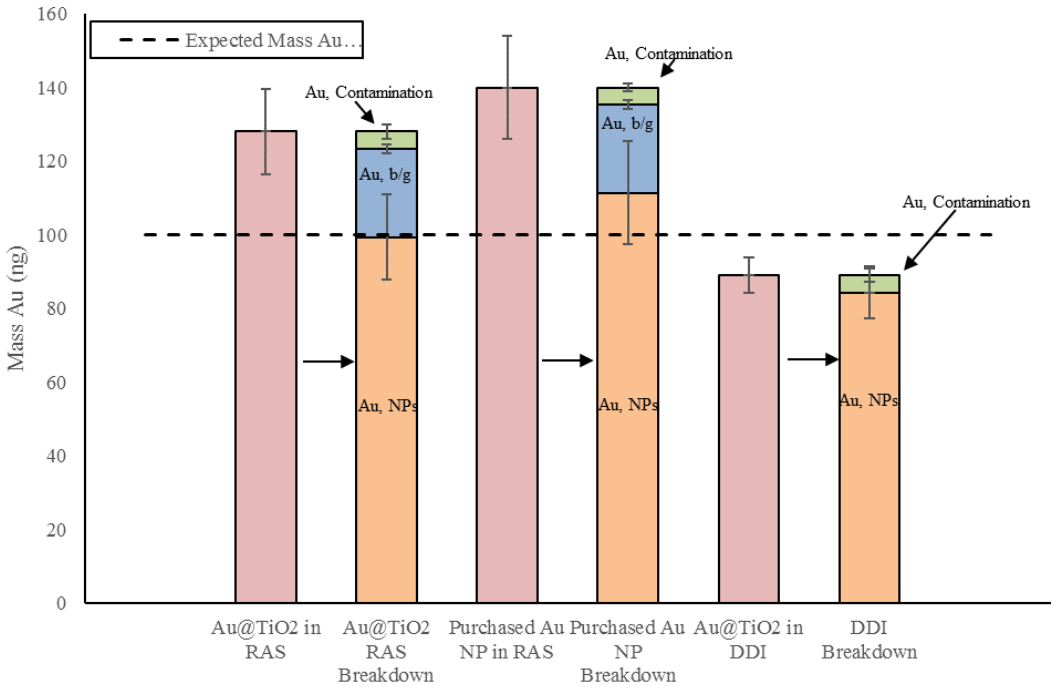

Figure 10. Mass Au measured in return activated sludge samples and DDI samples spiked with 100 ng Au from Au@TiO_2 nanoparticles, and their respective breakdown of Au sources. Also includes 100 ng of PEG capped Au NPs in RAS. Error bars represent a 95% confidence interval.

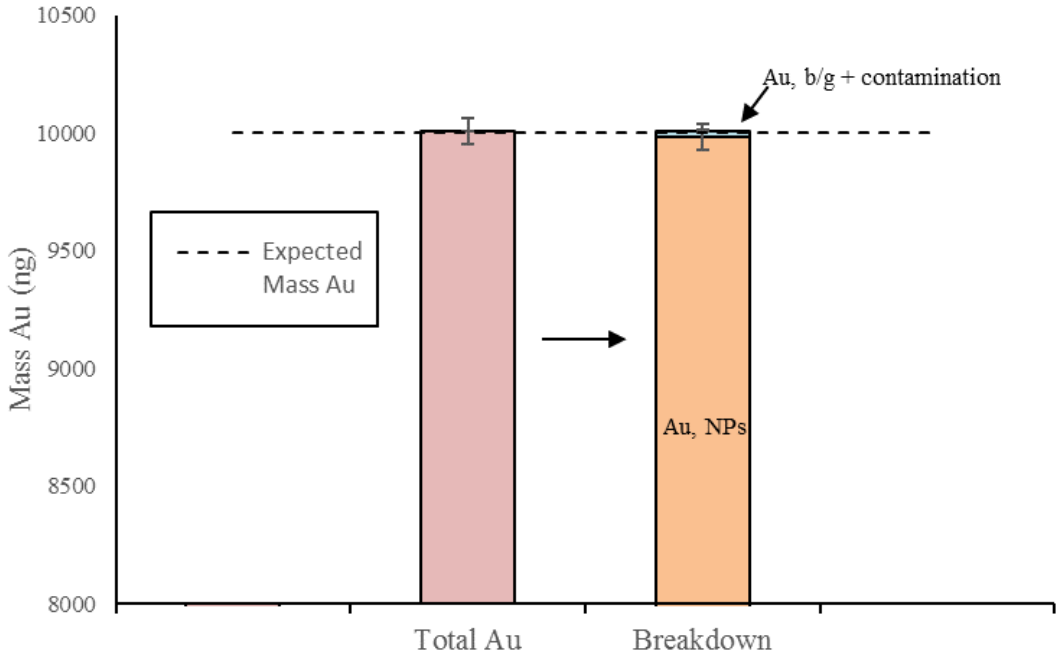

Figure 11 Mass Au measured in samples spiked with 10 µg Au from Au@TiO_2 nanoparticles in 1 mL return activated sludge, and the breakdown of Au sources. Note the y axis starts at 8,000 ng. Error bars represent 95% confidence intervals.

6.2 Zeta Potential of Au@TiO_2 nanoparticles

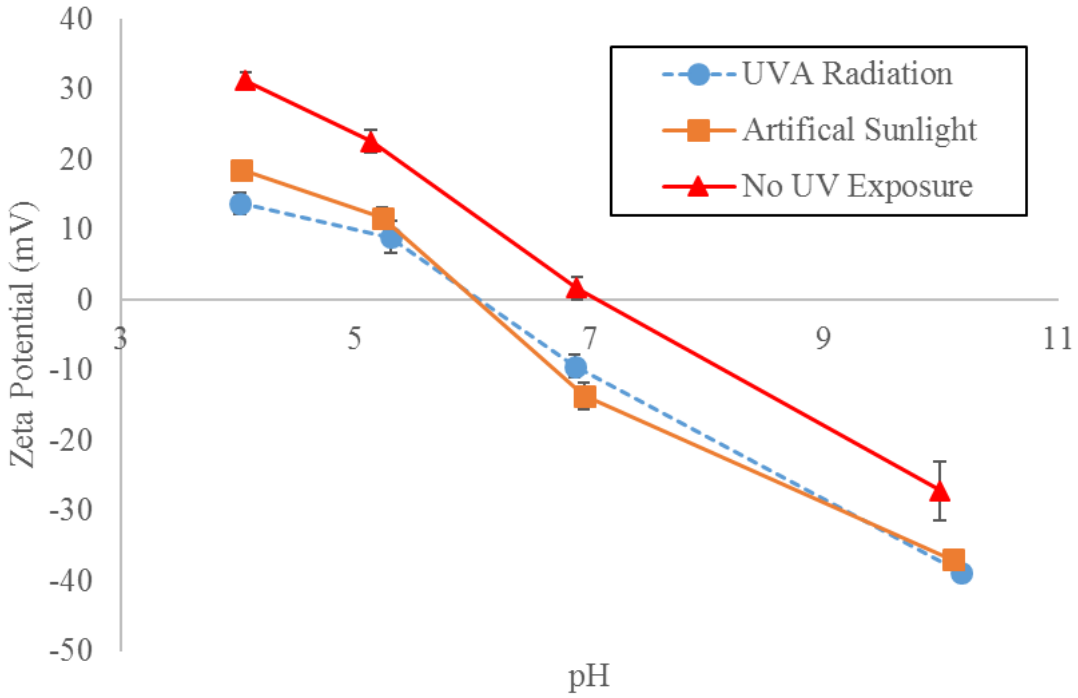

Figure 12 Calculated zeta potential of Au@TiO_2 nanoparticles. Error bars represent 95% confidence intervals. The conditions used to determine zeta potential are in Table 1.

Particle Size	245 nm
Surface Coating	Polyvinylpyrrolidone
Shape:	Spherical
Model:	Smoluchowski
pH	4, 5.3, 7, 10
Ionic Solution	1 mM KCl
Temperature	25°C
Viscocity	8.9×10^{-4} Pa s
Particle Concentration	10 ppm
Duration of Measurement	5 minutes
Number of measurements made	20
Number of replicate measurements	5

Table 1. Conditions used to determine zeta potential.

6.3 Batch Adsorption Test Supernatant Analysis

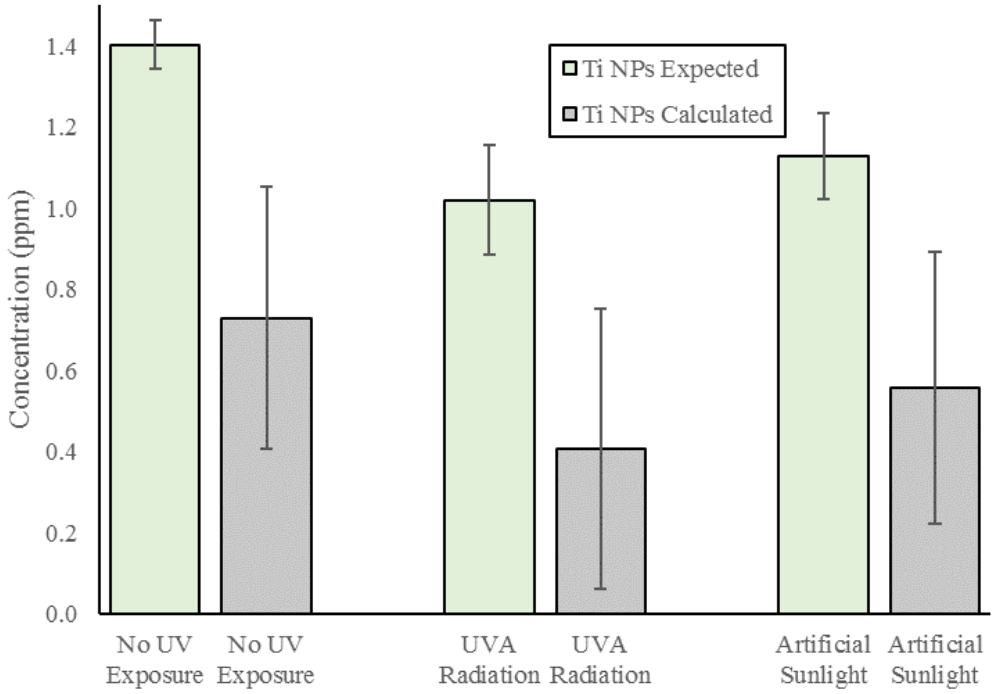

Figure 13. Calculated Ti associated with Au@TiO_2 nanoparticles compared to the expected amount of Ti associated with the nanoparticles in the supernatant of the batch adsorption tests. Assumes an Au:Ti ratio of the Au@TiO_2 nanoparticles of 1.29. Error bars represent 95% confidence interval.

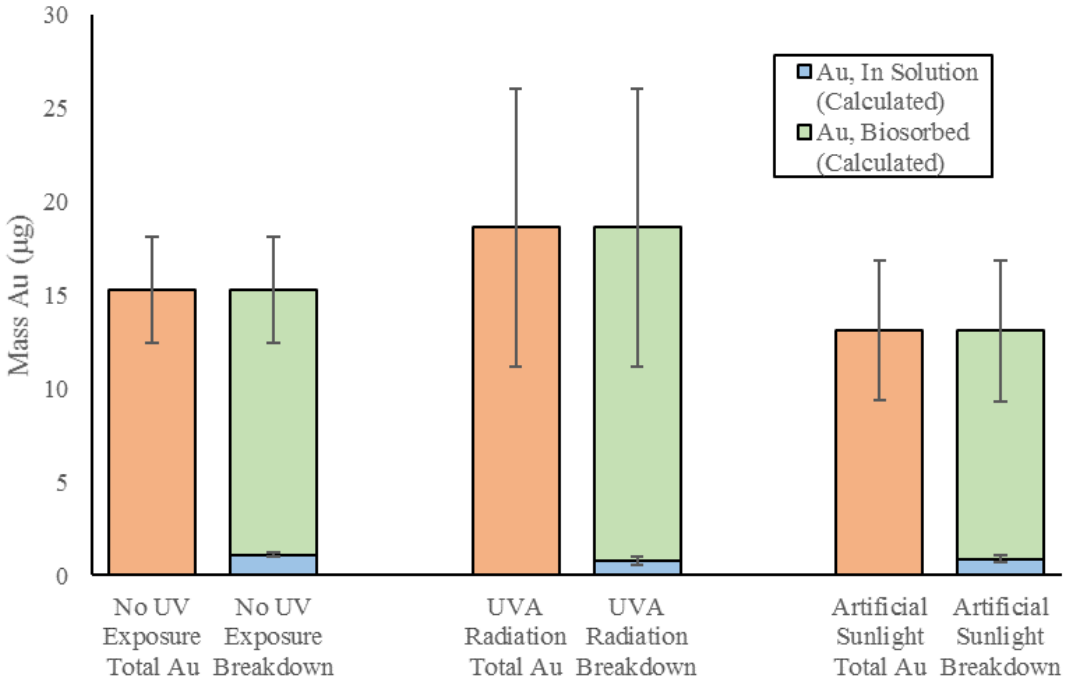

Figure 14. Total mass Au measured in settled solids, broken down into Au associated with the biosorption to heterotrophic biomass and suspended unattached Au in solution. Error bars represent 95% confidence intervals.

6.4 Calculations

Calculation of Au Background for RAS

Given

Au measured in 1 mL return activated sludge: 28.67 ng $\sigma_1 = 0.58$

Au measured associated with contamination: 4.67 ng $\sigma_2 = 1.00$

Calculate

Background concentration Au in return activated sludge

Solve

Average Value:

$$28.67 \text{ ng} - 4.67 \text{ ng} = 24.00 \text{ ng}$$

Error Propagation:

$$\sigma_1 = \sqrt{\sigma_1^2+\sigma_2^2} = \sqrt{0.58^2+1.00^2} = 1.15 \text{ ng}$$

$$24.0 \pm 1.2 \text{ ng}$$

Au Content of Dried RAS

Given

TSS of RAS:	5358 mg/L	$\sigma_1 = 577$ mg/L
Mass Au in 1 mL RAS	24.0 ng	$\sigma_2 = 1.2$

Calculate

Concentration Au in dried RAS

Solve

$$\frac{(24.0 \text{ ng})(\frac{1 \text{ µg}}{1000 \text{ ng}})}{(5358 \frac{\text{mg}}{\text{L}})(0.001\text{L})(\frac{\text{kg}}{1\times10^6 \text{mg}})} = 4479.3 \text{ µg/kg}$$

Error Propagation

$$\sigma_a = (a)\sqrt{(\frac{\sigma_1}{x_1})^2+(\frac{\sigma_2}{x_2})^2} = (4779.3)\sqrt{(\frac{577}{5358})^2+(\frac{1.2}{24.0})^2} = 531.8 \text{ µg/kg}$$

$$4479.3 \pm 531.8 \text{ µg/kg}$$

Limit of Detection

Given
Mass Au in 1 mL RAS 24.0 ng σ_2 =1.15

Calculate
The limit of detection of Au using INAA

Solve
Assume 95% confidence, two sided

$$LOD = \text{Mean Blank} + \text{Stdev Blank} \times 3.30$$

$$LOD = 24.0\ ng + 1.15\ ng \times 3.30$$

$$\boxed{LOD = 27.8\ ng}$$

Limit of Quantification

Given
Mass Au in 1 mL RAS 24.0 ng σ_2 =1.15

Calculate
The limit of quantification of Au using INAA

Solve
Assume 95% confidence, two sided

$$LOQ = \text{Mean Blank} + \text{Stdev Blank} \times 3.30$$

$$LOQ = 24.0\ ng + 1.15\ ng \times 10$$

$$\boxed{LOQ = 35.5\ ng}$$

Sample Calculation for Determining AuNP Content (10 ng Au)

Given

Total Au Measured	46.0 ng	$\sigma_1 = 1.00$ ng
Au from Contamination	4.67 ng	$\sigma_2 = 1.00$ ng
Au from Background	24.0 ng	$\sigma_2 = 1.15$ ng

Calculate

Au associated with $Au@TiO_2$ NPs

Solve

$$128.0 \text{ ng} - 4.67 \text{ ng} - 24.0 \text{ ng} = 17.3 \text{ ng}$$

Error Propagation

$$\sigma = \sqrt{\sigma_1^2+\sigma_2^2 + \sigma_2^2}=\sqrt{1.00^2+1.00^2 + +1.15^2}=1.82 \text{ ng}$$

Confidence Interval

$$\frac{(1.82 \text{ ng})(4.30)}{\sqrt{3}}=4.30$$

Mass Au from $Au@TiO_2$ NPs: $\boxed{17.3 \pm 4.30 \text{ ng}}$

Hypothesis Test Comparing Calculated Au from NPs to 10 ng

Given
Mass Au from Au@TiO_2 NPs = 17.3 ng σ = 1.82 ng
μ=17.3, μ_o = 10

Null Hypothesis
$\mu = \mu_o$

Solve

$$t = \frac{\mu - \mu_o}{\frac{\sigma}{\sqrt{n}}}$$

$$t = \frac{17.3\text{-}10}{\frac{1.82}{\sqrt{3}}} = 6.968$$

p(t=6.97, df=2)=0.020

0.020 < 0.05

$p < \alpha$

The null hypothesis is rejected.

Terminal Settling Velocity of 245 nm Nanoparticle

Given
d_p = 245 nm 2.45 x 10^{-7} m

Assume
g = 9.806 m/s^2
ρ_p = 4310 kg/m^3
ρ_p = 1000 kg/m^3
μ = 8.90 x 10^{-4} Pa. s

Find
v_t

Solve

$$v_t = \frac{g(\rho_p - \rho_w)d_p^2}{18\mu} = \frac{9.806\ \frac{m}{s^2}(4310\ \frac{kg}{m^3} - 1000\ \frac{kg}{m^3})(2.45 \times 10^{-7}\ m)^2}{(18)(8.90 \times 10^{-4}\ \frac{kg}{s\ m})}$$

v_t = 4.96 x 10^{-8} m/s

7 References

[1] Zhang, Y. Chen, Y., Westerhoff, P., Hristovski, K., Crittenden, J. "Stability of commercial metal oxide nanoparticles in water." *Water Research*. 42. 8-9 (2008): 2204-2212.

[2] Oberdorster, F., Penney, D. "Pulmonary Retention of Ultrafine and Fine Particles in Rats." *American Journal of Respiratory Cell and Molecular Biology*. 6.5 (1992): 535-542.

[3] Lowry, G., Gregory, K., Apte, S., Lead, J. "Transformations of nanomaterials in the environment." *Environmental Science and Technology*. 43.12 (2009): 4227-4233.

[4] Montazer, M., Seifollahzadeh, S. "Enhanced Self-cleaning, Antibacterial and UV Protection Properties of Nano TiO_2 Treated Textile through Enzymatic Pretreatment." *Photochemistry and Photobiology*, 87.4. (2011): 877-883.

[5] Robichaud, Christine Ogilvie, Ali Emre Uyar, Michael R. Darby, Lynne G. Zucker, and Mark R. Wiesner. "Estimates of Upper Bounds and Trends in Nano-TiO2Production as a Basis for Exposure Assessment." *Environmental Science & Technology* 43.12 (2009): 4227-233.

[6] Carp, O., C. L. Huisman, and A. Reller. "Photoinduced reactivity of titanium dioxide." *Progress in Solid State Chemistry* 32.1-2 (2004): 33-177.

[7] Pitkethly, Michael J. "Nanomaterials – the driving force." *Materials Today* 7.12 (2004): 20-29.

[8] Weir, A., Westerhoff, P., Fabricius, L., Goetz, N. "Titanium Dioxide Nanoparticles in Food and Personal Care Products." *Environmental Science and Technology*. 46.4 (2012): 2242-250.

[9] Gondikas, A., Kammer, F., Reed, R., Wagner, S., Ranville, J., Hofmann, T. "Release of TiO_2 Nanoparticles from sunscreens into surface waters: A one-year study at the old danube recreational lake." *Environmental Science and Technology*. 48 (2014): 5415-422.

[10] Tovar-Sanchez, A., et al. "Sunscreen Products as Emerging Pollutants to Costal Waters." *PLOS One*. (2013).

[11] Kaegi, R.; Ulrich, A.; Sinnet, B.; Vonbank, R.; Wichser, A.; Zuleeg, S.; Simmler, H.; Brunner, S.; Vonmont, H.; Burkhardt, M.; Boller, M. "Synthetic TiO_2 nanoparticle emission from exterior facades into the aquatic environment". *Environmental Pollution*. 156.2 (2008) 233–239.

[12] Keller, A., McFerran, S., Lazareva, A., Suh, S. "Global life cycle releases of engineered nanomaterials." *Journal of Nanoparticle Resources*. 15.1692 (2013).

[13] Praetorius, A., Scheringer, M., Hungerbuhler, K. "Development of environmental fate models for engineered nanoparticles-a case study of TiO_2 nanoparticles in the Rhine river." *Environmental Science and Technology*. 46 (2012): 6705-6713.

[14] Liu, X., Chen, G., Keller, A., Su, C. "Effects of dominant material properties on the stability and transport of TiO_2 nanoparticles and carbon nanotubes in aquatic environmentas: From synthesis to fate." *Environmental Science: Processes Impacts*. 15.1 (2013): 169-189.

[15] Zhu, X., Zhou, J., Cai, Z. "TiO_2 Nanoparticles in the Marine Environment: Impact on the Toxicity of Tributyltin to Abalone (*Haliotis diversicolor supertexta*) Embryos." *Environmental Science and Technology*. 45 3753-58. 2011

[16] Ma, H., Brennan, A., Diamond, S. "Phototoxicity of TiO_2 Nanoparticles under solar radiation to two aquatic species: *Daphnia manga* and Japanese medka." *Environmental Toxicology*. 31.7 (2012): 1621-1629.

[17] Zheng, X., Chen, Y., Wu, R. "Long-term effects of titanium dioxide nanoparticles on nitrogen and phosphorous removal from wastewater and bacterial community shift in activated sludge." *Environmental Science and Technology*. 45.17 (2011) 7284-7290.

[18] Madl, K., Pinkerton, K. "Health effects of inhaled engineered and incidental nanoparticles." *Critical Reviews in Toxicology*. 38.8 (2009): 629-658
.

[19] Sugibayashi, K., Todo, H., Kimura, E. "Safety evaluation of titanium dioxide nanoparticles by their absorption and elimination profiles." *The Journal of Toxicological Sciences*. 33.3 (2008): 293-298.

[20] Weir, A. *TiO_2 Nanomaterials: Human Exposure and Environmental Release*. MS Thesis. Arizona State University, 2011. Web.

[21] Gottschalk, F., Lassen, C., Kjoelholt, J., Christensen, F., Nowack, B. "Modeling flows and concentrations of nine engineered nanomaterials in the Danish environment." *International Journal of Environmental Research and Public Health*. 12.5 (2015): 5581-5602.

[22] Bitrangunta, S., Palani, S., Gopala, A., Sarkar, S., Kandukuri, V. "Detection of TiO_2 nanoparticles in Municiapl Sewage Treatment Plant and Their Characterization Using Single Particle ICP-MS." *Bulletin of Environmental Contamination and Toxicology*. 98.5 (2017) 595-600.

[23] Tong, T., Hill, A., Alsina, M., Wu, J., Shang, K., Kelly, J., Gray, K., Gaillard, J. "Spectroscoptic characterization of TiO_2 polymorphs in wastewater treatment and sediment samples." *Environmental Science and Technology Letters*. 2 (2015): 12-18.

[24] Westerhoff, P., Song, G., Hristovski, K., Kiser, M. "Occurrence and removal of titanium at full scale wastewater treatment plants: implications for TiO_2 nanomaterials." *Journal of Enviornmental Monitoring*. 13 (2011): 1195-1203.

[25] Luo, Z., Wang, Z., Li, Q., Pan, Q., Yan, C., Liu, F. "Spatial distribution, electron microscopy analysis of titanium and its correlation to heavy metals: occurrence and sources of titanium nanomaterials in surface sediments from Xiamen Bay, China." *Journal of Environmental Monitoring.* 13 (2011) 1046-1052.

[26] Acheampong, M., Antwi, D. "Modification of titanium dioxide for wastewater treatment application and its recovery for reuse." *Journal of Environmental Science and Engineering*. 5 (2016): 498-510.

[27] Praetorius, A., Tufenkji, N., Goss, K., Scheringer, M., Kammer, F., Elimelech, M. "The road to nowhere: equilibrium partition coefficients for nanoparticles." *Enviornmental Science: Nano*. 1 (2014): 317-323.

[28] Sheng, G., Zhang, L., Yu, H. "Characterization of adsorption properties of extracellular polymeric substances (EPS) extracted from sludge." *Colloids and Surfaces B: Biointerfaces*. 62.1 (2008): 83-90.

[29] Thill, A., Zeyons, O., Spalla, O., Chauvat, F., Rose, J., Auffan, M., Flank, A. "Cytotoxicity of CeO_2 nanoparticles for *Escherichia coli.* Physiochemical insights of the cytotoxicity mechanism." *Environmental Science and Technology*. 40 (2006): 6151-6156.

[30] Sahle-Demessie, E., Tadesse, H. "Kinetic and equilibrium adsorption of nano-TiO_2 paticles on synthetic biofilm." *Surface Science*. 605 (2011): 1177-1184.

[31] Patil, S., Sandberg, A., Heckert, E., Self, W., Seal, S. "Protein adsorption and cellular uptake of cerium oxide nanoparticles as a function of zeta potential." *Biomaterials*. 28.31 (2007): 4600-4607.

[32] Limach, L., Bereiter, R., Muller, E., Krebs, R., Galli, R., Stark, W. "Removal of oxide nanoparticles in a model wastewater treatment plant: influence of agglomeration and surfactants on clearing efficiency." *Environmental Science and Technology*. 42 (2008): 5828-5833.

[33] Chauque, E., Zvimba, J., Ngila, J., Musee, N. "Fate, behavior, and implications of ZnO nanoparticles in a simulated wastewater treatment plant." *Water SA*. 42.1 (2016).

[34] Mu, H., Chen, Y. "Long-term effect of ZnO nanoparticles on waste activated sludge anaerobic digestion." *Water Research*. 45.17 (2011): 5612-5620.

[35] Kiser, M., Ryu, H., Jang, H., Hristovski, K., Westerhoff, P. "Biosorption of nanoparticles to heterotrophic wastewater biomass." *Water Research*. 44.14 (2010): 4105-4114.

[36] Delay, M., Frimmel, F. "Nanoparticles in aquatic systems." *Analytical and Bioanalytical Chemistry*. 402 (2012): 583-592.

[37] Domingos, R., Tufenkji, N., Wilkinson, K. "Aggregation of titanium dioxide nanoparticles: role of a fulvic acid." *Environmental Science and Technology*. 43.5 (2009): 1282-1286.

[38] Keller, A., Wang, H., Zhou, D., Lenihan, H., Cherr, G., Cardinale, B., Miller, R., Ji, Z. "Stability and aggregation of metal oxide nanoparticles in natural aqueous matrices." *Environmental Science and Technology*. 44 (2010): 1962-1967.

[39] French, R., Jacobson, A., Kim, B., Isley, S., Penn, R., Baveye, P. "Influence of ionic strength, pH, and cation valence on aggregation kinetics of titanium dioxide nanoparticles." *Environmental Science and Technology*. 43 (2009): 1354-1359.

[40] Tkachenko, N., Yaremko, Z., Bellmann, C., Soltys, M. "The influence of ionic and nonionic surfactants on aggregative stability and electrical surface properties of aqueous suspensions of titanium dioxide." *Journal of Colloid and Interface Science*. 299.2 (2006): 686-695.

[41] Sun, P., Zhang, K., Fang, J., Lin, D., Wang, M., Han, J. "Transport of TiO_2 nanoparticles in soil in the presence of surfactants." *Science of the Total Environment*. 527-528 (2015): 420-428.

[42] Fang, J., Shan, X., Wen, B., Lin, J., Owens, G. "Stability of titania nanoparticles in soil suspensions and transport in saturated homogeneous soil columns." *Enviornmental Pollution*. 157.4 (2009): 1101-1109.

[43] Miller, R., Bennett, S., Keller, A., Pease, S., Lenihan, H. "TiO_2 Nanoparticles are Phototoxic to Marine Phytoplankton." *PLOS* 7.1 (2012).

[44] Lee, W., An, Y. "Effects of zinc oxide and titanium dioxide nanoparticles on green algae under visible, UVA and UVB radiations: No evidence of enhanced algal toxicity under UV pre-irradiation." *Chemosphere*. 91.4 (2013): 536-544)

[45] Li, S., Wallis, L., Diamond, S., Ma, H., Hoff, D. "Species sensitivity and dependence on exposure conditions impacting the phototoxicity of TiO_2 nanoparticles to benthic organisms." 33.7 (2014): 1563-1569.

[46] Bundschuh, M., Zubrod, J., Englert, D., Seitz, F., Rosenfeldt, R., Schulz, R. "Effects of nano-TiO_2 in combination with ambient UV-irradiation on a leaf shredding amphipod." *Chemosphere*. 85.10 (2011): 1563-1567.

[47] Lin, D., Tian, X., Wu, F., Xing, B. "Fate and transport of engineered nanomaterials in the environment." *Journal of Environmental Quality*. 36.6 (2009): 1896-1908.

[48] Wang, R., Hashimoto, K., Fujishima, A., Chikuni, M., Kojima, E., Kitamura, A., Shimolhigoshi, M., Watanabe, T. "Photodegredation of Highly amphiphilic TiO_2 surfaces." *Advanced Materials*. 10.2 (1998): 135-138.

[49] Hao, Y-Q., Wang, Y-F., Weng, Y-X. "Particle-size-dependent hydrophlicity of TiO_2 nanoparticles characterized by marcus reorganization energy of interfacial charge recombination." *Journal of Physical Chemistry C*. 112 (2008): 8995-9000.

[50] Thompson, T., Yates, J. "Surface Science Studies of the Photoactivation of TiO_2 – New photochemical processes." *Chemical Review*. 106 (2006): 4428-4453.

[51] Wang, R., Hashimoto, K., Fujishima, A., Chikuni, M., Kojima, E. "Light-induced amphiphilic surfaces." *Nature*. 338.6641 (1997): 431-432.

[52] Sun, J., Guo, L., Zhang, H., Zhao, L. "UV Irradiation induced transformation of TiO_2 nanoparticles in water: aggregation and photoreactivity." *Environmental Science and Technology*. 48 (2014): 11962-11968.

[53] Wang, P., Qui, N., Ao, Y., Hou, J., Wang, C., Qian, J. "Effect of UV irradiation on the aggregation of TiO_2 in an aquatic environment: influence of humic acid and pH." *Environmental Pollution*. 212 (2016): 178-187.

[54] Kiser, M., Westerhoff, P., Benn, T., Wang, Y., Perez-Rivera, J., Hristovski, K. "Titanium Nanomaterial Removal and Release from Wastewater Treatment Plants." *Environmental Science and Technology*. 43 (2009): 6757-763.

[55] Kammer, F., Ferguson, P., Holden, P., Masion, A., Rogers, K., Klaine, S., Koelmans, A., Hornes, N., Urines, Jason. "Analysis of engineered nanomaterials in complex matrices (environment and biota): General considerations and conceptual case studies." *Environmental Toxicology and Chemistry*. 31.1 (2012): 32-49.

[56] Eby, Nelson. "Instrumental neutron activation analysis (INAA)." *University of Massachusetts Lowell*. Web accessed 10 May, 2017.

[57] Oughton, D., Hertel-Aas, T., Pellicer, E., Mendoza, E., Joner, E. "Neutron activation of engineered nanoparticles as a tool for tracing their environmental fate and uptake in organisms." *Nanomaterials in the environment*. 27.9 (2008): 1883-1887.

[58] Glascock, D.M.D. "Overview of Neutron Activation Analysis. *University of Missouri Research Reactor*. Web accessed 10 May, 2017.

[59] Westerhoff, P., Lee, S., Yang, Y., Gordon, G., Hristovski, K., Halden, R., Herckes, P. "Characterization, recovery opportunities, and valuation of metals in municipal sludges from U.S. wastewater treatment plants nationwide." *Environmental Science and Technology*. 46.16 (2015): 9479-9488.

[60] Harper, S., Carriere, J., Miller, J., Hutchison, J., Maddux, B., Tanguay, R. "Systemic Evaluation of nanomaterial toxicity: utility of standardized materials and rapid assays." *ACS Nano*. 5.6 (2011): 4688-4697.

[61] Balogh, et. al. "Significant effect of size on the in vivo biodistribution of gold composite nanodevices in mouse tumor models." *Nanomedecine: Nanotechnology, Biology, and Medicine*. 3 (2007) 281-296.

[62] McBride, M., Richards, B., Steenhuis, T., Russo, J., Sauve, S. "Mobility and solubility of toxic metals and nutrients in soil fifteen years after sludge application." *Soil Science*. 162.7 (1997): 487-500.

[63] Deline, A., Young, W., Nason, J. "Synthesis and utility of gold core labeled TiO_2 nanoparticles for tracking behavior in complex matrices."

[64] Goebl, J., Joo, J., Dahl, M., Yin, Y. "Synthesis of tailered Au@TiO_2 core-shell nanoparticles for photocatalytic reforming of ethanol." *Catalysis Today*. 225 (2014): 90-95.

[65] Doktorovova, S., Shegokar, R., Martins-Lopes, P., Silva, A., Lopes, C., Muller, R., Souto, E. "Modified rose Bengal assay for surface hydrophobicity evaluation of cationic solid lipid nanoparticles (cSLN). *European Journal of Pharmaceutical Sciences*. 45 (2012): 606-612.

[66] APHA, AWWA, and WEF. *Standard methods for the examination of water and wastewater*. Washington D.C.: American Public Health Association, 2005. Print

[67] Amiel, S., *Nondestructive Activation Analysis*. Yavne: Elsevier Scientific Publishing Company, 1981. 238-239.

[68] Fang, L. *Method Development for Characterizing the Hydrophobicity of Engineered Nanoparticles*. MS Thesis. Oregon State University, 2013. Web.

[69] Xiao, Y., Wiesner, M. "Characterization of surface hydrophobicity of engineered nanoparticles." *Journal of Hazardous Materials*. 215-216 (2012): 146-151.